



**US Army Corps  
of Engineers**

Waterways Experiment  
Station

Contract Report W-94-1  
July 1994

*Water Quality Research Program*

## **A Model of Manganese and Iron Fluxes from Sediments**

*by Dominic M. Di Toro, James F. Fitzpatrick, Richard R. Isleib  
HydroQual, Inc.*



Approved For Public Release; Distribution Is Unlimited

# **A Model of Manganese and Iron Fluxes from Sediments**

by Dominic M. Di Toro, James F. Fitzpatrick, Richard R. Isleib

HydroQual, Inc.  
One Lethbridge Plaza  
Mahwah, NJ 07430

**Final report**

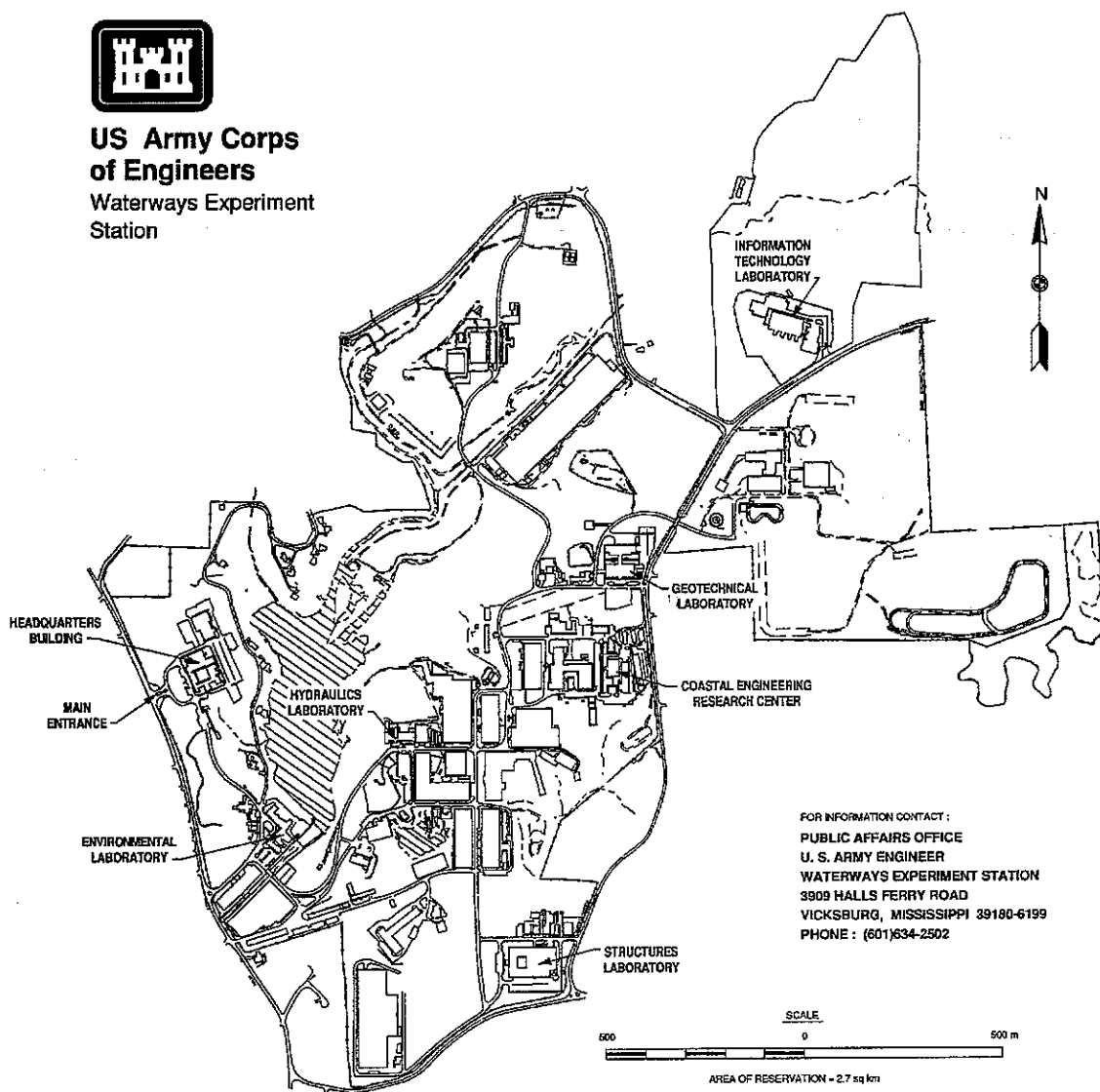
Approved for public release; distribution is unlimited

Prepared for U.S. Army Corps of Engineers  
Washington, DC 20314-1000

Monitored by U.S. Army Engineer Waterways Experiment Station  
3909 Halls Ferry Road, Vicksburg, MS 39180-6199



**US Army Corps  
of Engineers**  
Waterways Experiment  
Station



**Waterways Experiment Station Cataloging-in-Publication Data**

Di Toro, Dominic M.

A model of manganese and iron fluxes from sediments / by Dominic M. Di Toro, James F. Fitzpatrick, Richard R. Isleib ; prepared for U.S. Army Corps of Engineers ; monitored by U.S. Army Engineer Waterways Experiment Station.

76 p. : ill. ; 28 cm. -- (Contract report ; W-94-1)

Includes bibliographical references.

1. Marine sediments -- Composition -- Mathematical models.
  2. Chemical oceanography -- Long Island Sound (N.Y. and Conn.)
- I. Fitzpatrick, James F. II. Isleib, Richard R. III. United States. Army. Corps of Engineers. IV. U.S. Army Engineer Waterways Experiment Station. V. Water Quality Research Program. VI. Title. VII. Series: Contract report (U.S. Army Engineer Waterways Experiment Station) ; W-94-1.

TA7 W34c no.W-94-1

# Contents

---

Preface . . . . .	iv
I—Introduction . . . . .	1
II—Chemistry . . . . .	2
III—Partitioning Model of Manganese Fluxes . . . . .	7
IV—Calcium-Alkalinity Flux Model . . . . .	17
V—Manganese-Calcium-Alkalinity Flux Model . . . . .	27
VI—Application to MERL Data . . . . .	48
VII—References . . . . .	59
Appendixes I-IV	
SF 298	

# Preface

---

The work reported herein was conducted as part of the Water Quality Research Program (WQRP), Work Unit 32694. The WQRP is sponsored by the Headquarters, U.S. Army Corps of Engineers (HQUSACE), and is assigned to the U.S. Army Engineer Waterways Experiment Station (WES) under the purview of the Environmental Laboratory (EL). Funding was provided under Department of the Army Appropriation No. 96X3121, General Investigation. The WQRP is managed under the Environmental Resources Research and Assistance Programs (ERRAP), Mr. J. L. Decell, Manager. Mr. Robert C. Gunkel, Jr., was Assistant Manager, ERRAP, for the WQRP. Technical Monitors during this study were Mr. Frederick B. Juhle, Mr. Rixie Hardy, and Dr. John Bushman.

Principal Investigators of the work unit were Drs. Carl Cerco, Water Quality and Contaminant Modeling Branch (WQCMB), Environmental Processes and Effects Division (EPED), EL, and Douglas Gunnison, Ecosystem Processes and Effects Branch (EPEB), EPED.

The report was prepared by Dr. Dominic Di Toro and Messrs. James Fitzpatrick and Richard Isleib of HydroQual, Inc., Mahwah, NJ. Technical review was provided by Dr. Cerco and Mr. Gene Ploskey, WQCMB. Preparation of the report was under the general supervision of Dr. Mark S. Dortch, Chief, WQCMB, Dr. Richard E. Price, Chief, EPEB, Mr. Donald L. Robey, Chief, EPED, and Dr. John W. Keeley, Director, EL.

At the time of publication of this report, Director of WES was Dr. Robert W. Whalin. Commander was COL Bruce K. Howard, EN.

This report should be cited as follows:

Di Toro, D. M., Fitzpatrick, J. F., and Isleib, R. R. (1994).  
"A model of manganese and iron fluxes from sediments,"  
Contract Report W-94-1, U.S. Army Engineer Waterways  
Experiment Station, Vicksburg, MS.

*The contents of this report are not to be used for advertising, publication, or promotional purposes. Citation of trade names does not constitute an official endorsement or approval of the use of such commercial products.*

## I. Introduction

The purpose of this report is to present the progress that has been made in the development of a model of manganese and iron fluxes from sediments. It is based on the sediment model (Di Toro and Fitzpatrick, 1993) developed for the Chesapeake Bay water quality model (Cерco and Cole, 1993). This report assumes that the reader has a familiarity with the concepts and formulations developed therein.

This report concentrates on the development the manganese flux model. As shown below, the chemistry of iron and manganese are sufficiently similar so that it is expected that this model formulation can be applied to either.

Two manganese data sets have been located, one of which is quite substantial. The equivalent data for iron, which includes aerobic fluxes as well as anaerobic fluxes, does not appear to be available. Since the manganese data is much larger and more interesting it appears reasonable to use these sets for the initial development.

## II. Chemistry

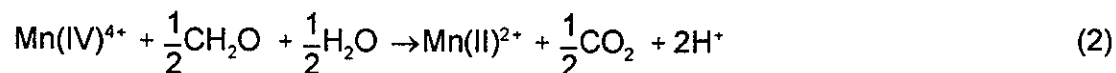
### A. Manganese

#### 1. Species and Redox Transformations

The chemistry of manganese in natural waters and sediments has been studied for quite some time [Stumm and Morgan, 1970]. Manganese exists in two valences states: Mn(II) in anoxic waters and Mn(IV) in oxic waters. Mn(IV) is very insoluble and forms manganese oxide,  $\text{MnO}_2(\text{s})$ , which is the predominant form of manganese in oxic surface waters. It usually exists as a coating on particles [Jenne, 1968]. As the particles settle to the sediment, manganese is also transported providing a source of manganese to the sediments. In the oxic layer of the sediment,  $\text{MnO}_2(\text{s})$  is stable. However, particle mixing causes particles to be transported to the anaerobic layer of the sediment where manganese oxide is thermodynamically unstable and a reduction reaction occurs. Mn(IV) is reduced to Mn(II). For this to occur, two electrons are required as can be seen from the following half reaction:



Thus the reaction requires an electron donor. The primary source of electrons in sediments is organic matter,  $\text{CH}_2\text{O}$ , so that the reduction reaction can be written:



This reaction follows from the half reaction for oxygen:



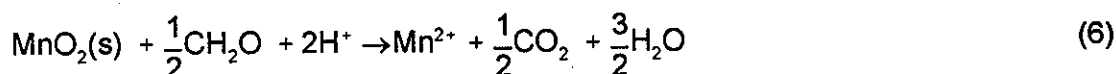
and the oxygen equivalents of organic matter:



Since it is actually  $\text{MnO}_2(\text{s})$  that is being reduced, the substitution of the equation corresponding to the formation of  $\text{MnO}_2(\text{s})$  yields:



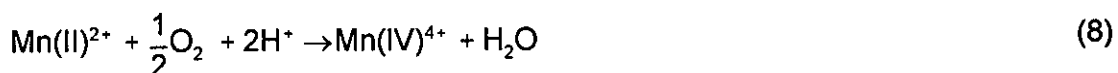
so that the complete reduction reaction of manganese oxide to  $\text{Mn(II)}$  is:



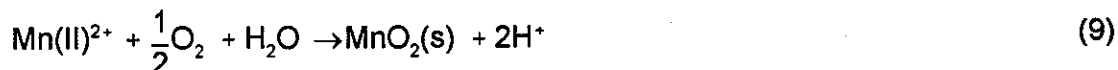
In contrast to  $\text{Mn(IV)}$ ,  $\text{Mn(II)}$  is more soluble and exists in the mg/L range in sediment pore waters. As a consequence it can diffuse to the oxic layer of the sediment where it is subject to oxidation. The oxidation of  $\text{Mn(II)}$  to  $\text{Mn(IV)}$  occurs via the loss of two electrons:



For oxygen as the electron acceptor, the overall reaction can be found using the half reaction for oxygen, eq.(3),:



followed by the precipitation of manganese oxide, eq.(5):



This is the reaction that occurs in the aerobic layer. The kinetics of this reaction have been examined [Morgan, 1967] and found to be slow in the normal pH ranges of surface waters. However the reaction can be bacterially mediated and proceed more rapidly [Jaquet et al., 1982].



## 2. Solubility

In oxic waters, Mn(IV) is very insoluble and manganese oxide,  $\text{MnO}_2(\text{s})$ , is the predominant species. In anoxic waters, two solid phase species may exist: manganese carbonate,  $\text{MnCO}_3(\text{s})$  (rhodocrosite), and manganese sulfide,  $\text{MnS}(\text{s})$ . Since iron sulfide is also present in sediments, and it is more insoluble than  $\text{MnS}(\text{s})$ , it is unlikely that manganese sulfide is present. We will assume below that the solubility of Mn(II) is controlled by  $\text{MnCO}_3(\text{s})$ . Thus not all of the Mn(II) that is formed by the reduction of  $\text{MnO}_2$  is in dissolved form. Some of it precipitates to form manganese carbonate. Therefore the transfer of Mn(II) from the anoxic to the oxic layer occurs via particle mixing which transports  $\text{MnCO}_3(\text{s})$  as well as diffusion of soluble Mn(II).

### B. Iron

#### 1. Species and Redox Transformations

Like manganese, the chemistry of iron in natural waters and sediments has also been studied for quite some time [Stumm and Morgan, 1970]. Iron exists in two valences states: Fe(II) in anoxic waters and Fe(III) in oxic waters. Fe(III) is very insoluble and forms iron oxyhydroxide,  $\text{FeOOH}(\text{s})$ . Like manganese, it usually exists as a coating on particles. However, unlike manganese, there are other forms of iron that exist as particles in natural waters. Since the crust is approximately two percent iron, particles that runoff into natural waters contain a large amount of iron. As the particles settle to the sediment, iron is transported as well. This is the source of iron to the sediments.

Not all iron is reactive in sediments. It is convenient to denote the reactive portion of oxic iron as  $\text{FeOOH}(\text{s})$  (Goethite), and to assume that it includes iron hydroxide as well since:

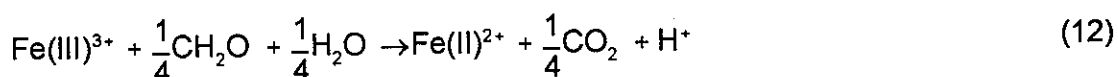


The term iron oxyhydroxide is meant to denote the sum of  $\text{FeOOH}(\text{s})$  and  $\text{Fe}(\text{OH})_3(\text{s})$ .

In the oxic layer of the sediment, FeOOH(s) is stable. However, as particle mixing causes particles to be transported into the anaerobic layer of the sediment, iron oxyhydroxide is thermodynamically unstable and a reduction reaction occurs. Fe(III) is reduced to Fe(II). For this to occur, one electron is required as can be seen from the following half reaction:



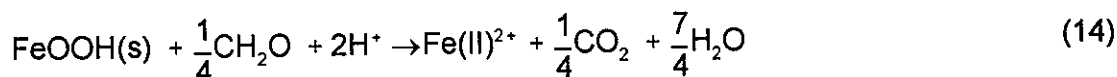
Thus it requires an electron donor. Again the source of electrons in sediments is organic matter, CH<sub>2</sub>O. Thus the reduction reaction can be written:



This reaction follows from eq.(3-4) and eq.(11). Since it is actually FeOOH(s) that is being reduced, the substitution of the equation corresponding to the formation of FeOOH(s):



yields:

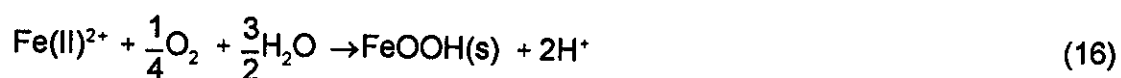


as the final reduction reaction of iron oxyhydroxide to Fe(II).

By contrast to Fe(III), Fe(II) is more soluble and exists in the low mg/L range in sediment pore waters. As a consequence it can diffuse to the oxic layer of the sediment where it is subject to oxidation. The oxidation of Fe(II) to Fe(III) occurs via the loss of one electron which is the reverse of eq.(11). With oxygen as the electron acceptor, the overall reaction can be found using the half reaction for oxygen, eq.(3),



followed by the precipitation of iron oxyhydroxide, eq.(13) to yield the overall reaction:



This is the reaction that occurs in the aerobic layer. The kinetics of this reaction have been examined and found to be slow in the normal pH ranges of surface waters. However, like manganese oxidation, this reaction can also be bacterially mediated and proceed more rapidly.

Thus the chemistry of manganese and iron are quite similar. The oxidized forms are both insoluble and form oxides. The reduced forms are soluble in the mg/L range. Their concentrations in pore water are regulated by solid phases. Their flux to the overlying water is controlled by the extent that the reduced forms are oxidized in the aerobic layer, or escape as fluxes. Responses to lowered dissolved oxygen appear to be similar (Sunby et al., 1986). Hence it is expected that the formulations for manganese developed below can be applied to iron.

### III. Partitioning Model of Manganese Fluxes

#### A. Model Formulation

The model structure is shown in Fig.3.1. It is formulated in terms of manganese but to equally applies to iron since the mechanisms are analogous. There are four dependent variables: Mn(II) and MnO<sub>2</sub>(s) in layers 1 and 2. These correspond to the total Mn(II) and Mn(IV) in each layer. The source of manganese to the sediment is the settling of particulate manganese oxide with flux,  $J_{\text{MnO}_2}$ , from the overlying water. Two reactions occur in the aerobic layer. Mn(II) partitions to form manganese carbonate. The reaction is parameterized with a linear partition coefficient,  $\pi_1$ . In addition, Mn(II) is oxidized to MnO<sub>2</sub>(s) following eq.(9) with first order rate,  $k_{\text{Mn},1}$ .

Two reactions also occur in the anaerobic layer. Mn(II) partitions to form manganese carbonate which is parameterized with a linear partition coefficient,  $\pi_2$ . This may be different from  $\pi_1$  in the aerobic layer due to the differences in pH and alkalinity. In addition, MnO<sub>2</sub>(s) is reduced to Mn(II) following eq.(6) with first order rate,  $k_{\text{Mn},2}$ .

The mass transport between the overlying water and layer one is via the surface mass transfer coefficient,  $K_{\text{L}01}$ , which is set equal to  $s = \text{SOD}/\text{O}_2(0)$ , the ratio of the sediment oxygen demand and the overlying water dissolved oxygen concentration, as in the previous models (Di Toro and Fitzpatrick, 1993). Particle mixing with mixing velocity  $w_{12}$  and diffusive exchange with mass transfer coefficient  $K_{\text{L}12}$  are included as before, as is burial with sedimentation velocity  $w_2$ .

#### B. Equations and Solutions

The mass balance equations for the model follow from the reactions and transport processes discussed above. They are:

# MANGANESE FLUX MODEL

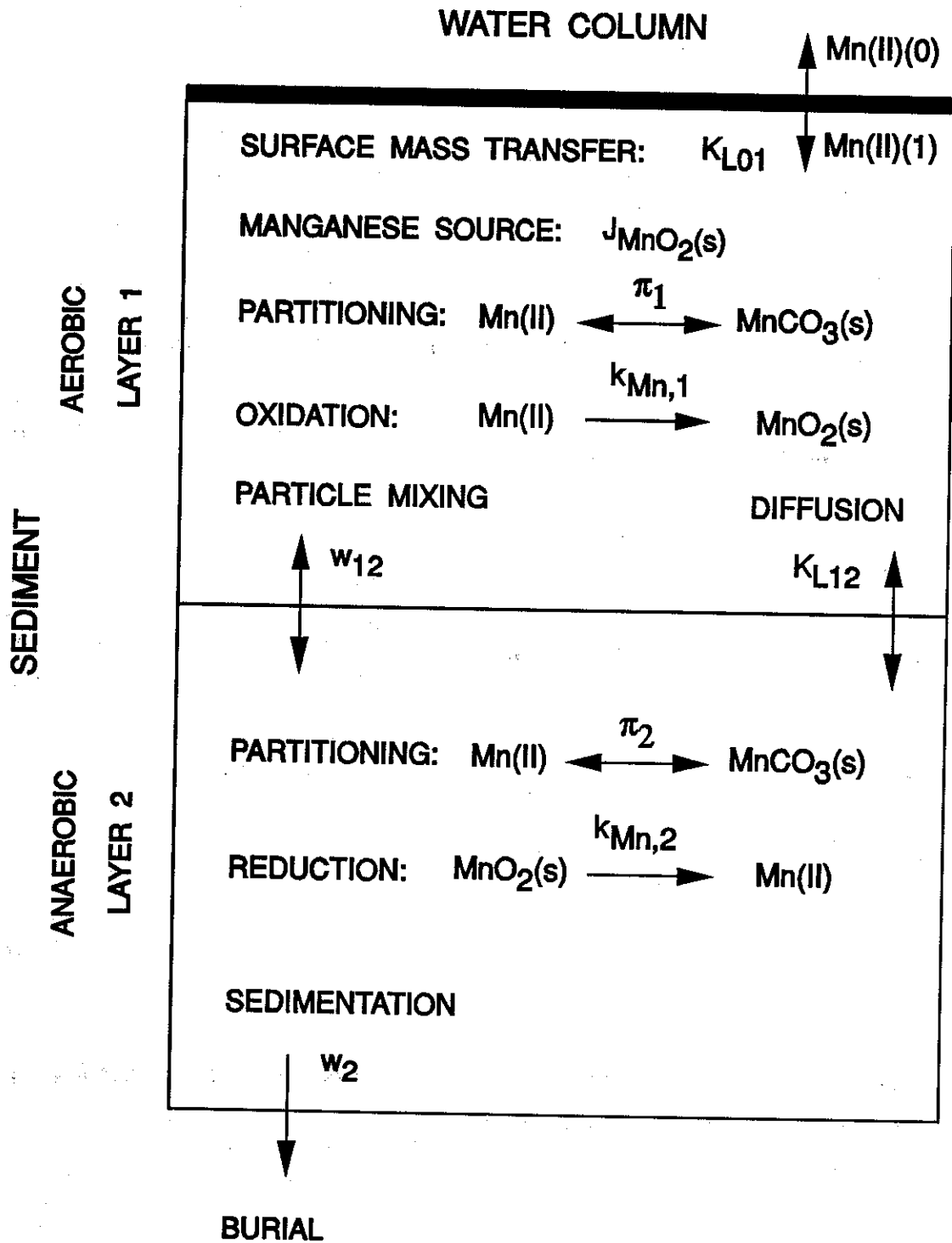


Figure 3.1

Layer 1 Mn(II):

$$0 = H_1 \frac{dMn(1)}{dt} = -s(f_{d1}Mn(1) - Mn(0)) + K_{L12}(f_{d2}Mn(2) - f_{d1}Mn(1)) + w_{12}(f_{p2}Mn(2) - f_{p1}Mn(1)) - k_{Mn,1}f_{d1}Mn(1) \quad (17)$$

Layer 2 Mn(II):

$$0 = H_2 \frac{dMn(2)}{dt} = -K_{L12}(f_{d2}Mn(2) - f_{d1}Mn(1)) - w_{12}(f_{p2}Mn(2) - f_{p1}Mn(1)) - w_2Mn(2) + k_{Mn,2}MnO_2(2) \quad (18)$$

Layer 1 MnO<sub>2</sub>:

$$0 = H_1 \frac{dMnO_2(1)}{dt} = k_{Mn,1}f_{d1}Mn(1) + w_{12}(MnO_2(2) - MnO_2(1)) + J_{MnO_2} \quad (19)$$

Layer 2 MnO<sub>2</sub>:

$$0 = H_2 \frac{dMnO_2(2)}{dt} = -k_{Mn,2}MnO_2(2) - w_{12}(MnO_2(2) - MnO_2(1)) - w_2MnO_2(2) \quad (20)$$

where the particulate and dissolved fractions are computed from the partition coefficients and the concentration of solids,  $m$ , in each layer:

$$f_d = \frac{1}{1 + m\pi} = 1 - f_p \quad (21)$$

The solutions to these steady state equations are:

$$Mn(2) = \frac{J_{MnO_2} k_{Mn,2}}{w_2^2 f_{d1} k_{Mn,2} s r_{12} + w_2 (r_{12} (k_{Mn,1} + f_{d1} s) + k_{Mn,2})} \quad (22)$$

where:

$$r_{12} = \frac{f_{d2} K_{L12} + f_{p2} w_{12}}{f_{d1} (K_{L12} + s) + k_{Mn,1} + f_{p1} w_{12}} \quad (23)$$

The layer 1 solutions is:

$$Mn(1) = r_{12} Mn(2) \quad (24)$$

and the manganese flux is:

$$J[Mn] = s (f_{d1} Mn(1) - Mn(0)) \quad (25)$$

This model will be compared to observations in the next section.

### C. Manganese Flux Data

Two data sets will be examined using this model. This first is a relatively small number of manganese and nutrient flux measurements made at three Long Island Sound stations (Aller, 1980). The second is a large number of manganese (Hunt and Kelly, 1988) and nutrient flux measurements made at the MERL mesocosms (Nixon et al., 1986). The analysis technique is to examine the relationship between observed and computed ammonia,  $J[NH_4]$ , and the manganese,  $J[Mn]$ , fluxes. As shown in Fig.3.2 there is a proportional relationship between these two fluxes.

# Manganese and Ammonia Flux

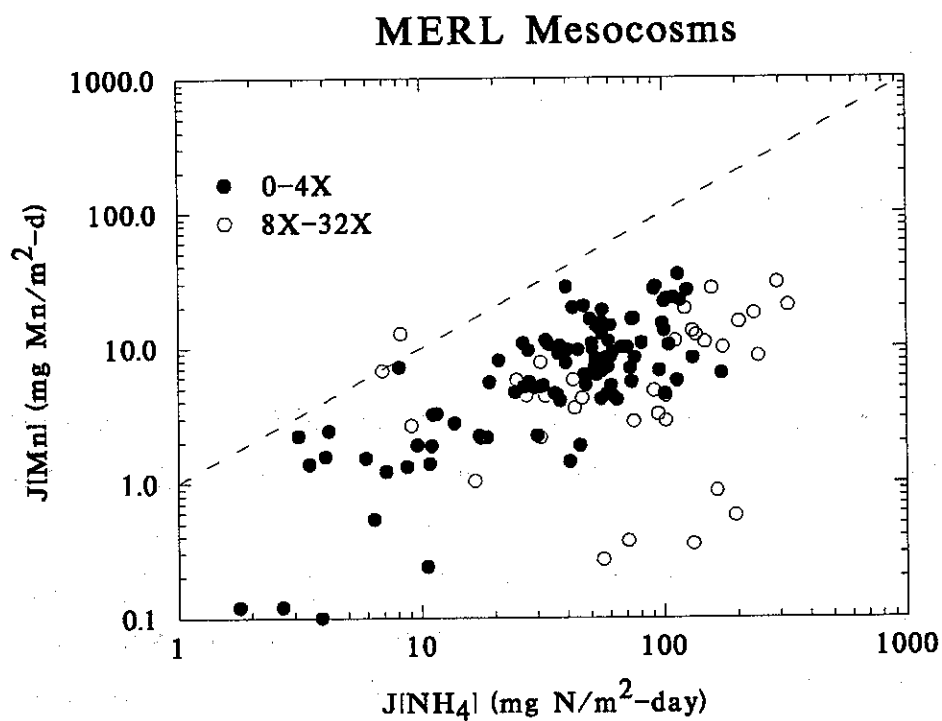
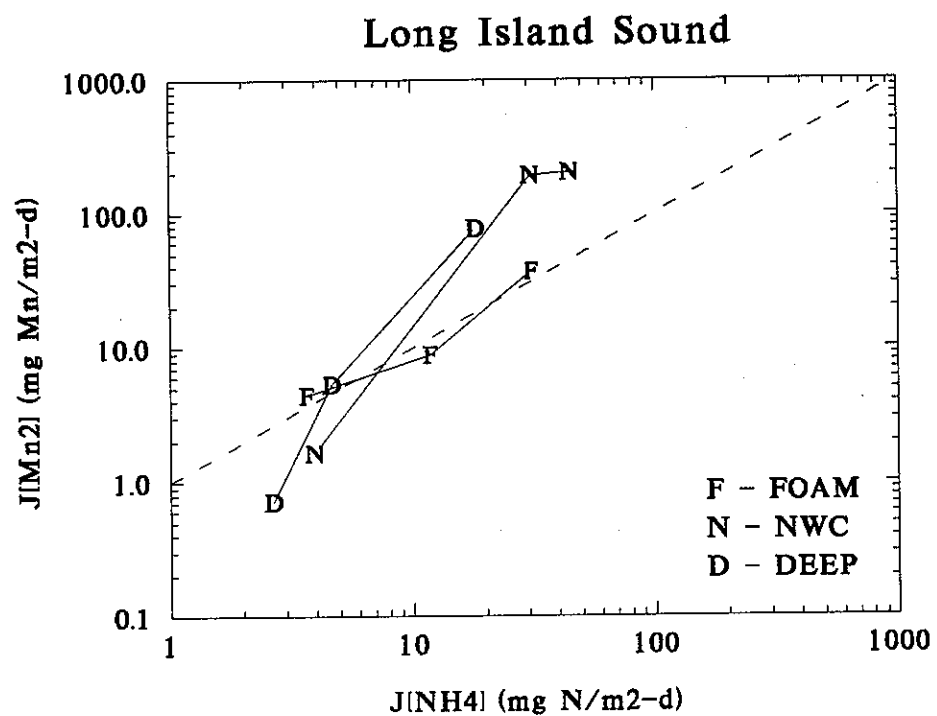


Figure 3.2



## 1. Relationship between $J[\text{NH}_4]$ and SOD

The parameter in the manganese model equations that depends on the ammonia flux is the surface mass transfer coefficient:  $s = \text{SOD}/\text{O}_2(0)$ . This parameter controls both the rate of mass transfer from the sediment to the overlying water and the depth of the aerobic layer,  $H_1$ . As  $s$  increases, one would expect that  $J[\text{Mn}]$  would increase since both the rate of surface mass transfer increases, and the depth of the aerobic zone decreases. The latter effect decreases the residence time in the aerobic layer and makes the oxidation of  $\text{Mn(II)}$  to  $\text{MnO}_2(\text{s})$  less rapid, enabling more  $\text{Mn(II)}$  to escape to the overlying water.

The dependency of  $s$  on ammonia flux occurs because the ammonia flux and SOD are related. This can be seen from the following equations. The steady state relationship between ammonia diagenesis,  $J_N$  and ammonia flux,  $J[\text{NH}_4]$  is (Di Toro and Fitzpatrick, 1993):

$$J[\text{NH}_4] = J_N \frac{s^2}{s^2 + K_{\text{NH}_4}^2} \quad (26)$$

where the effect of the overlying water ammonia concentration is assumed to be small. At steady state, nitrogen diagenesis can be estimated using SOD and the Redfield ratio:

$$\text{SOD} = a_{\text{O}_2, \text{N}} J_N \quad (27)$$

where  $a_{\text{O}_2, \text{N}}$  is the Redfield ratio between  $\text{O}_2$  and nitrogen. Since:

$$s = \text{SOD}/\text{O}_2(0) \quad (28)$$

$s$  can be estimated from ammonia flux by solving these equations for  $s$  as a function of  $J[\text{NH}_4]$ .

This provides the necessary connection. Using eqs.(26-28), the relationship between ammonia diagenesis,  $J_N$ , ammonia flux,  $J[NH_4]$  and SOD is:

$$J_N = \frac{1}{3} \left[ \frac{(2 a_{O_2,N}^2)^{1/3} J[NH_4]^2}{d_1} + J[NH_4] + \frac{d_1}{(2 a_{O_2,N}^2)^{1/3}} \right] \quad (29)$$

where:

$$d_1 = [ 2a_{O_2,N}^2 J[NH_4]^3 + 27 J[NH_4] \kappa_{NH_4,1}^2 O_2(0)^2 + 3^{3/2} J[NH_4] \kappa_{NH_4,1} O_2(0) ( 4 a_{O_2,n}^2 J[NH_4]^2 + 27 \kappa_{NH_4,1}^2 O_2(0)^2 )^{1/2} ]^{1/3} \quad (30)$$

This approximation assumes that all carbon diagenesis eventually becomes SOD, i.e. that losses due to sulfide fluxes and burial are negligible. From an analysis of Chesapeake Bay fluxes, these losses amount to no more than 25%. The second source of error is due to the time lags that occur between the production of oxygen equivalents by carbon diagenesis and their eventual oxidation. These are caused by the formation and the subsequent oxidation of  $FeS(s)$ . From an analysis of steady state version of the sediment model it is known that the time lag effect causes an error of approximately a factor of two between the carbon diagenesis estimated from SOD assuming steady state, and the actual flux (Fig.5.4, Di Toro and Fitzpatrick 1993). Thus although these errors are not negligible, the approximations can be used so long as the magnitude of the error involved is understood.

#### D. Comparison to Data

The model computations are compared to the Long Island Sound data in Fig.3.3. The model parameters are listed in Table 1 and the computer program in the MATLAB language that produced the results is listed in Appendix I. The model predicts an

# Manganese Linear Partitioning Model

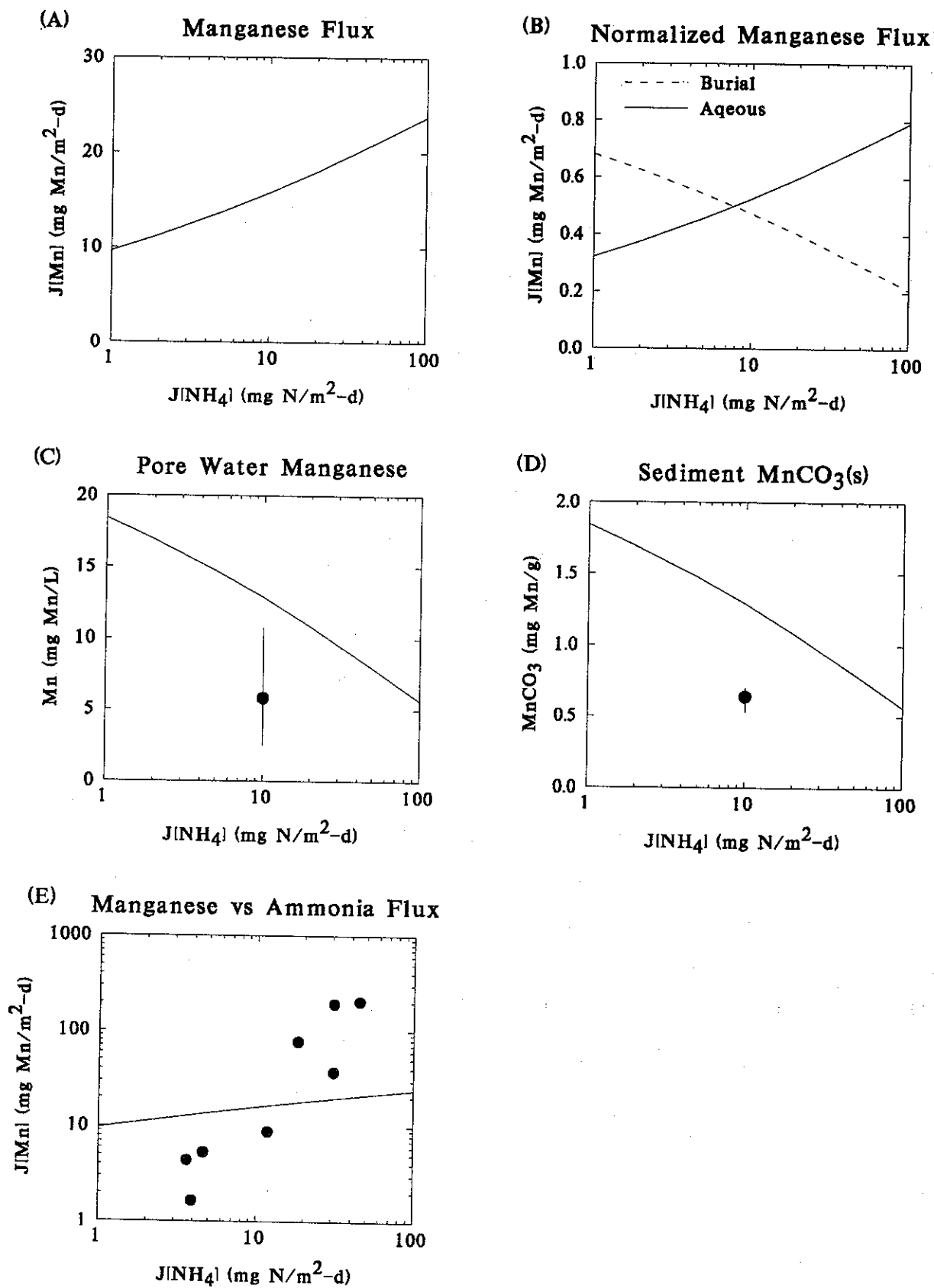


Figure 3.3

increasing flux of manganese as ammonia flux increases, Fig.(3.3a). As ammonia flux, and therefore  $s$  increases, less manganese is buried and, therefore, more escapes as a flux to the overlying water. The partition coefficient can be adjusted so that the observed particulate and dissolved manganese concentrations in the anaerobic layer can be reproduced. The data are plotted arbitrarily at an ammonia flux of  $10 \text{ mg N/m}^2\text{-day}$ . The model reproduces the concentrations at the higher ammonia flux., Fig.(3.3c-d). However, it is clear that the model cannot reproduce the magnitude of the observed  $J[\text{Mn}] - J[\text{NH}_4]$  relationship, Fig(3.3e). The discrepancy - almost two orders of magnitude - is too large to be attributed to the error associated with using  $s$  estimated from  $J[\text{NH}_4]$ . Therefore an important mechanism is missing in the linear partitioning model.

## E. Conclusions

The linear partitioning model cannot reproduce the observed relationship between manganese and ammonia fluxes. At steady state, there are only two possible pathways for manganese: either it escapes as a flux, or it is buried. Therefore, in order for the model to reproduce the observations it is necessary that it predicts a higher degree of burial at low ammonia fluxes and a larger manganese flux to the overlying water at high ammonia fluxes.

Perhaps the problem is with the linear partitioning assumption. The fraction of manganese that is particulate in the anaerobic layer is determined by the solubility of  $\text{MnCO}_3(\text{s})$ . This is not a linear partitioning process. Rather it is controlled by a chemical equilibrium between manganese and carbonate ion concentrations. In order to model this process, it is necessary to model the processes that control the carbonate concentration in sediments. A model for this process is discussed in the next section.

Table 1

## Parameter Values for Linear Partitioning Model

$m_1$	1.0	kg/L
$m_2$	1.0	kg/L
$K_{L12}$	0.01	m/d
$w_{12}$	0.012	m/d
$w_2$	0.25	cm/yr
$\pi_1$	100	L/kg
$\pi_s$	10,000	L/kg
$k_{Mn,1}$	1.0	m/d
$k_{Mn,2}$	1.0	m/d
$\kappa_{NH41}$	0.15	m/d
$O_2(0)$	5.0	mg/L
$a_{O2,N}$	2.54*5.68	mg $O_2$ /mg N
$J_{MnO2}$	100	mg Mn/m <sup>2</sup> -d

#### IV. Calcium - Alkalinity Flux Model

Most freshwater and marine sediments contain a large concentration of calcium carbonate. Typical values are 10 - 100 mg  $\text{CaCO}_3/\text{g}$  or 1 to 10% of the dry weight, so that there is as much inorganic carbon as there is organic carbon in sediments. This quantity of calcium carbonate provides a large buffer system for both the pH and the carbonate concentration in sediment pore water. The objective of the model formulated in the section is to reproduce the observations of pore water and solid phase concentrations of calcium and alkalinity.

##### A. Chemistry and Simplifications

A model of a chemical system is specified by the components in the model, and the species formed by the components (Morel, 1983). This applies to systems that are open (Di Toro, 1976), i.e. subject to mass transport, as well as the normal closed system considered in typical chemical calculations. The calcium carbonate system is well understood and is specified by three components: calcium, alkalinity, and total inorganic carbon. However, using three components results in an equation set that is too complex to be solved conveniently. Therefore a simplified set of components and equations are required.

The equation that determines the solubility of calcium carbonate is:

$$[\text{Ca}^{2+}][\text{CO}_3^{2-}] = K_{\text{sp}, \text{CaCO}_3} \quad (31)$$

The concentration of  $\text{Ca}^{2+}$  can be approximated with the concentration of total dissolved calcium, Ca. This ignores the complexes of calcium with bicarbonate and other ligands. The concentration of carbonate can be approximated using the definition of alkalinity:

$$[\text{Alk}] = [\text{HCO}_3^-] + 2[\text{CO}_3^{2-}] + [\text{OH}^-] - [\text{H}^+] \quad (32)$$

which in the pH range of sediment pore waters (pH = 7 - 8) and for large enough alkalinity,  $[\text{Alk}] > 0.1 \text{ meq/L}$ , is well approximated by:

$$[\text{Alk}] = [\text{HCO}_3^-] \quad (33)$$

The reaction between  $\text{HCO}_3^-$  and  $\text{CO}_3^{2-}$  is:



and the mass action law is:

$$\frac{[\text{HCO}_3^-]}{[\text{H}^+][\text{CO}_3^{2-}]} = K_2 \quad (35)$$

or:

$$\frac{[\text{Alk}]}{[\text{H}^+][\text{CO}_3^{2-}]} = K_2 \quad (36)$$

so that:

$$[\text{CO}_3^{2-}] = \frac{[\text{Alk}]}{K_2 [\text{H}^+]} \quad (37)$$

Thus the solubility mass action equation becomes:

$$\frac{[\text{Ca}][\text{Alk}]}{K_2 [\text{H}^+]} = K_{\text{sp, CaCO}_3} \quad (38)$$

or:

where  $K_{\text{CaAlk}}$  is the apparent solubility constant. Note that the effect of decreasing pH, which increases  $\text{H}^+$ , increases the apparent solubility constant, as it should since  $[\text{CO}_3^{2-}]$  is

$$[\text{Ca}][\text{Alk}] = K_{\text{sp,CaCO}_3} K_2 [\text{H}^+] \equiv K_{\text{CaAlk}} \quad (39)$$

decreasing as pH decreases.

This simplification reduces the number of components to two: Ca and Alk, and requires only that the pH be specified. This is a significant reduction in the complexity of the equations that need to be solved.

For a simple closed system, the mass balance equations are:

$$[\text{Ca}] + [\text{CaAlk}] = \text{Ca}_T \quad (40)$$

$$[\text{Alk}] + 2 [\text{CaAlk}] = \text{Alk}_T \quad (41)$$

The two in the alkalinity equation arises from the two equivalents of alkalinity in each mole of  $\text{CaCO}_3(\text{s})$ .  $\text{Ca}_T$  and  $\text{Alk}_T$  are the total concentrations of calcium and alkalinity in the system. Substituting these equations into the mass action eq.(39) yields:

$$(\text{Ca}_T - \text{CaAlk}) (\text{Alk}_T - 2 \text{CaAlk}) = K_{\text{CaAlk}} \quad (42)$$

which is a quadratic equation that is solved for CaAlk. This is then substituted in eqs.(40-41) to determine Ca and Alk.

## B. Sediment Model Equations and Solutions

The model formulation is shown in Fig.4.1. The dependent variables are: Alk(1) and Alk(2), the total alkalinity in layer 1 and layer 2 respectively; Ca(1) and Ca(2), the total calcium in the same sequence; and CaAlk(2), the calcium carbonate in layer 2. The mass balance and mass action equations are as follows.



# CALCIUM FLUX MODEL

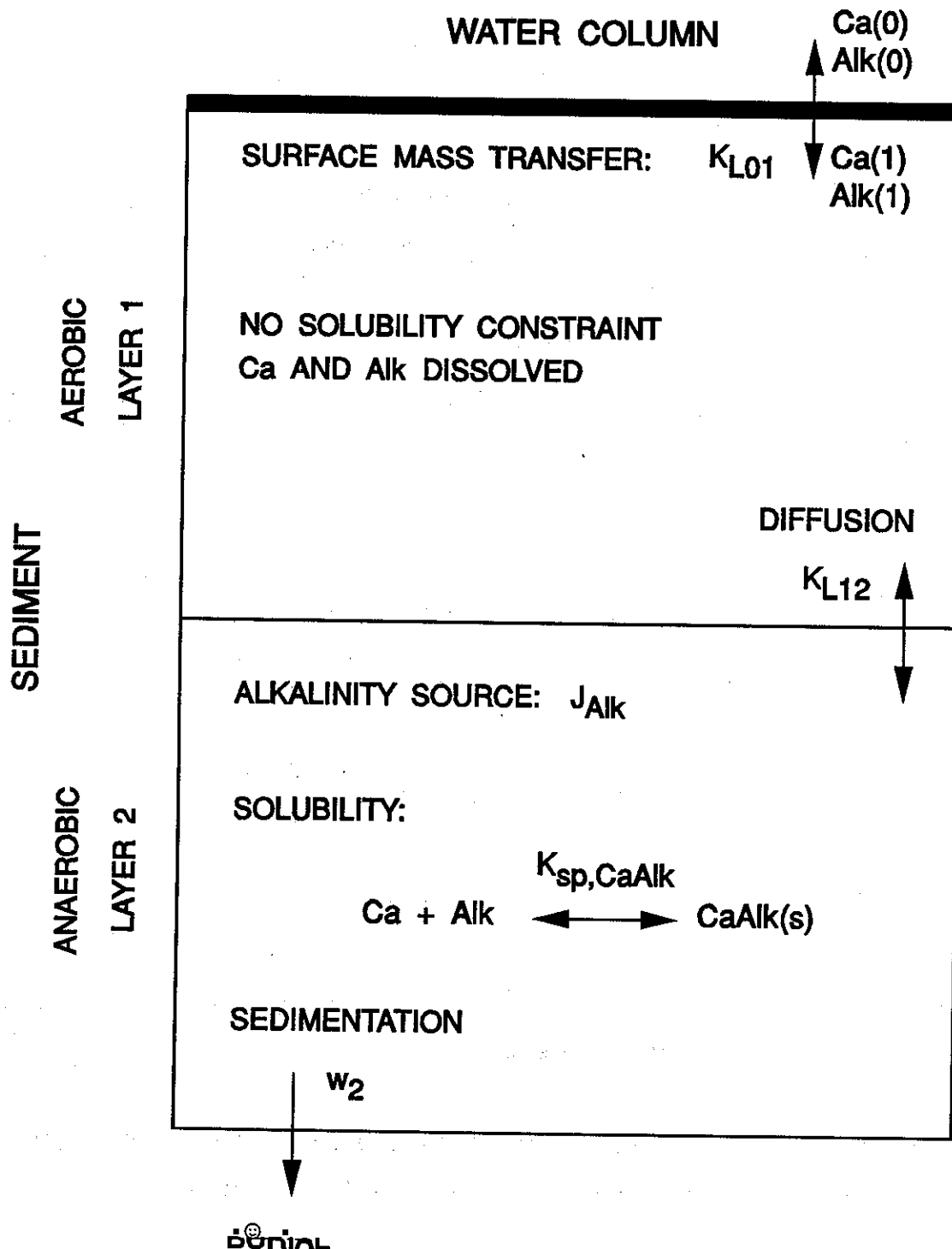


Figure 4.1

Layer 1 Alkalinity:

$$0 = s ( \text{Alk}(0) - \text{Alk}(1) ) + K_{L12} ( \text{Alk}(2) - 2 \text{CaAlk}(2) - \text{Alk}(1) ) \quad (43)$$

Layer 2 Alkalinity:

$$0 = -K_{L12} ( \text{Alk}(2) - 2 \text{CaAlk}(2) - \text{Alk}(1) ) - w_2 ( 2 \text{CaAlk}(2) ) + J_{\text{Alk}} \quad (44)$$

Layer 1 Calcium:

$$0 = s ( \text{Ca}(0) - \text{Ca}(1) ) + K_{L12} ( \text{Ca}(2) - \text{CaAlk}(2) - \text{Ca}(1) ) \quad (45)$$

Layer 2 Calcium:

$$0 = -K_{L12} ( \text{Ca}(2) - 2 \text{CaAlk}(2) - \text{Ca}(1) ) - w_2 ( \text{CaAlk}(2) ) \quad (46)$$

CaCO<sub>3</sub> Solubility

$$( \text{Ca}(2) - \text{CaAlk}(2) ) ( \text{Alk}(2) - 2 \text{CaAlk}(2) ) = K_{\text{CaAlk}} \quad (47)$$

where:

$$K_{\text{CaAlk}} = K_{\text{sp,CaCO}_3} K_2 [\text{H}^+] \quad (48)$$

is the apparent solubility product. The terms:  $\text{Ca}(2) - \text{CaAlk}(2)$  and  $\text{Alk}(2) - 2 \text{CaAlk}(2)$  are the dissolved calcium and alkalinity in layer 2.

The solution to these equations can be found as follows. The variables:  $\text{Alk}(1)$ ,  $\text{Alk}(2)$ ,  $\text{Ca}(1)$ , and  $\text{Ca}(2)$  are eliminated from the five simultaneous equations.

The resulting equation for CaAlk(2) is a quadratic equation of the form:

$$a \text{CaAlk}(2)^2 + b \text{CaAlk}(2) + c = 0 \quad (49)$$

where:

$$a = 2 (s + K_{L12})^2 w_2^2 \quad (50)$$

$$b = -(s + K_{L12}) ((2 \text{Ca}(0) + \text{Alk}(0)) K_{L12} s + J_{\text{Alk}} (s + K_{L12})) w_2 \quad (51)$$

$$c = -K_{L12} s ((K_{\text{CaAlk}} - \text{Alk}(0) \text{Ca}(0)) K_{L12} s - J_{\text{Alk}} \text{Ca}(0) (s + K_{L12})) \quad (52)$$

The computer code that implements these equations is given in Appendix 3.

It is remarkable that the solution to these five simultaneous equations is reduced to the solution of a quadratic equation, as it is for the simple closed system. This suggests that so long as the chemistry can be simplified to the point that the equations for a closed system are solvable, then the open system equations can also be solved.

### C. Application to Long Island Sound

The data for this application comes from observations of fluxes from three stations in Long Island Sound (Aller, 1980a, 1980b). The parameters required for the calcium - alkalinity flux model are the usual transport parameters as well as those specific to these components. These are listed in Table 2. The computer program that produced the results is listed in Appendix II.

In addition to the source of alkalinity from the overlying water there is also a sediment source of alkalinity. This is computed from an ammonia flux using the equations given above to obtain  $s$  and  $J_N$ . Redfield stoichiometry is used to compute the carbon

diagenesis,  $J_C$ . It is assumed that all carbon diagenesis reduces sulfate to sulfide following the formula:



Therefore each mole of organic carbon reacted produces one equivalent of bicarbonate alkalinity.

The only chemical parameter required for the model is the apparent solubility of CaAlk. Fig.4.2 presents the pore water data for dissolved calcium, Ca, and alkalinity, Alk, from three Long Island Sound stations. The product:  $[\text{Ca}][\text{Alk}]$  is also presented. It ranges from approximately  $20 \text{ (mM)}^2$  to over  $40 \text{ (mM)}^2$ . This sets the range for  $K_{\text{CaAlk}}$ .

With the parameters established, the model is evaluated by specifying an ammonia flux and computing the resulting concentrations. The additional parameter values are presented in Table 2.

Table 2

Parameter Values for the Calcium Carbonate Model

Ca(0)	326	mg Ca/L
Alk(0)	91.8	mg $\text{CaCO}_3$ /L
$K_{\text{sp}, \text{CaCO}_3}$	10 - 30	$\text{mM}^2$

## 1. Results

Fig.4.3 presents the results for  $K_{\text{CaAlk}} = 10 - 30 \text{ (mM)}^2$ . Alkalinity increases as ammonia flux increases, Fig.4.3a. For  $K_{\text{CaAlk}} = 30 \text{ (mM)}^2$  the solubility of CaAlk is exceeded

## Long Island Sound Pore Water

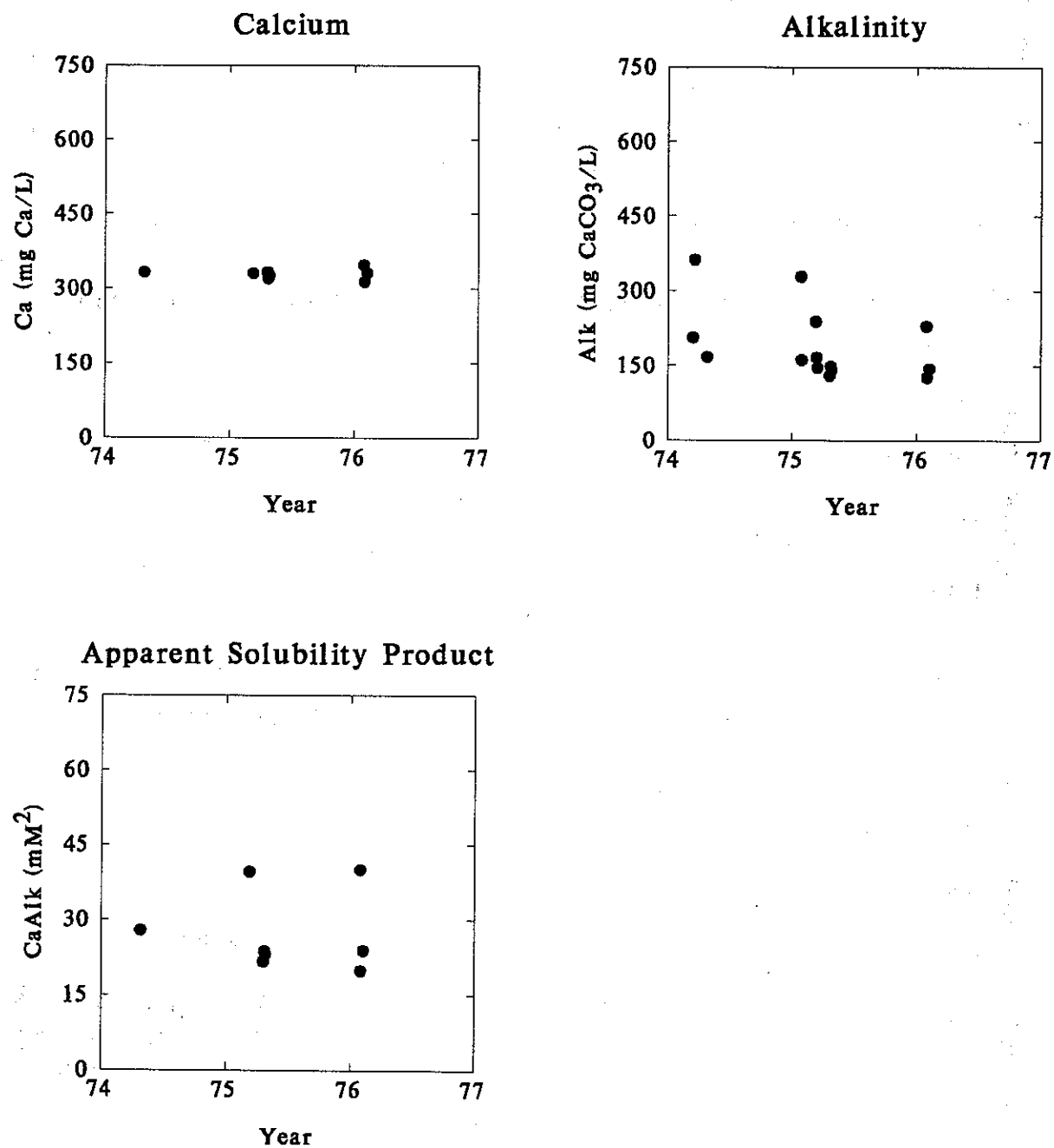


Figure 4.2

# Calcium - Alkalinity Model

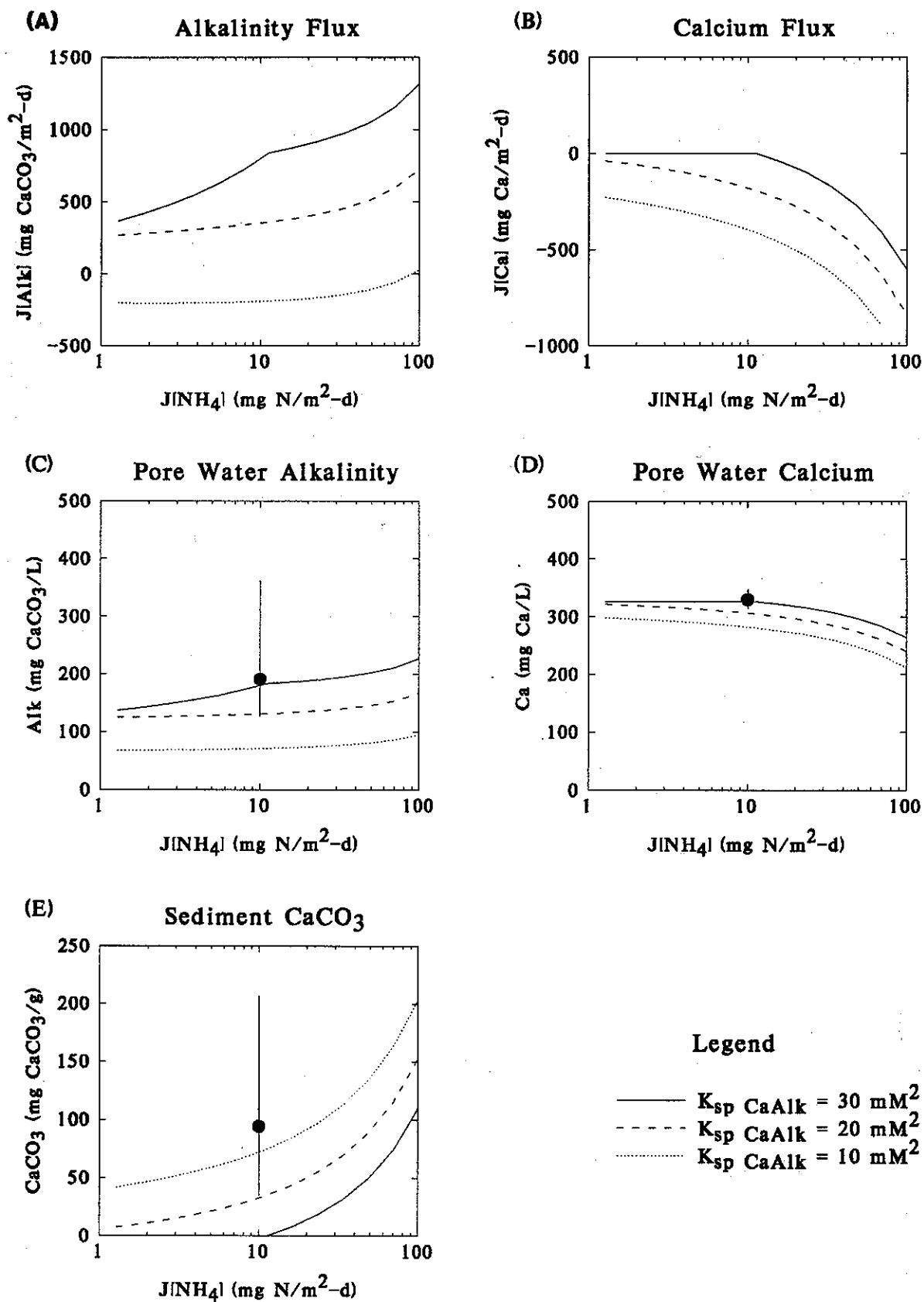


Figure 4.3

for  $J[\text{NH}_4] > 10 \text{ mg N/m}^2\text{-d}$  and  $\text{CaCO}_3(\text{s})$  starts to form, Fig 4.3e. At that point the calcium flux changes from zero to negative, Fig.4.3b, which is the flux into the sediment that is required to support the burial of  $\text{CaCO}_3$ . Also the flux of alkalinity from the sediment to the overlying water increases less rapidly, Fig.4.3a, since a portion is being buried. For smaller solubility products,  $K_{\text{CaAlk}} = 10 - 20 (\text{mM})^2$ ,  $\text{CaCO}_3(\text{s})$  forms over the entire range of  $J[\text{NH}_4]$  investigated, Fig.4.3e, and therefore calcium flux is to the sediment, Fig.4.3b.

Pore water concentrations are compared in Fig.4.3c-d. The data is plotted at  $J[\text{NH}_4] = 10 \text{ mg N/m}^2\text{-d}$  for convenience only. The annual average ammonia flux is somewhat larger. Alkalinity and calcium are reproduced for  $K_{\text{CaAlk}} = 30 (\text{mM})^2$ . Calcium concentrations are essentially equal to the overlying water concentrations whereas the alkalinity is larger, due to the additional source that results from sulfate reduction.

The concentration of  $\text{CaCO}_3(\text{s})$  is computed to increase from less than 10 mg  $\text{CaCO}_3/\text{g}$  (1% of dry weight) to over 100 mg  $\text{CaCO}_3/\text{g}$  (10%). Long Island Sound sediments contain between 25 and 200 mg/g. The model reproduces the observations of the lower values of the solubility constant. This is in contrast to the pore water results. Perhaps there is an additional source of calcium carbonate to the sediments, e.g,  $\text{CaCO}_3(\text{s})$  from bivalve shells, which accounts for the additional  $\text{CaCO}_3(\text{s})$ .

Nevertheless, the model is reasonably successful in reproducing the general features of the data. Pore water calcium concentrations are predicted to be close to the overlying water value, 326 mg/L, whereas alkalinity is predicted to be larger than the overlying value of 100 mg/L. Calcium carbonate concentrations are predicted to be in the range of 10 to 100 mg/g which is the range of the observations. These results are obtained using transport parameters that are calibrated from Chesapeake Bay sediment flux data, suggesting that these parameters are representative for these Long Island Sound sediments. In particular, the sedimentation velocity for these sediments is quite close to 0.5 cm/yr used for these calculations.

## V. Manganese - Calcium - Alkalinity Flux Model

A model is formulated in which the pore water and solid phase concentration of manganese are controlled by the solubility of manganese carbonate. To this end, the calcium carbonate model is included as part of the formulation. The rest of the model parallels the linear partitioning model presented in Section III.

### A. Chemistry and Simplifications

The simplification of the manganese chemistry parallels that for calcium. The concentration of  $\text{Mn(II)}^{2+}$  is approximated with the concentration of total dissolved manganese, Mn. This ignores the complexes of manganese with bicarbonate and other ligands. The concentration of carbonate can be approximated using alkalinity as formulated in section III. The mass action law for the solubility of  $\text{MnCO}_3(\text{s})$  is:

$$[\text{Mn}] [\text{Alk}] = K_{\text{sp, MnCO}_3} K_2 [\text{H}^+] = K_{\text{MnAlk}} \quad (54)$$

Pore water data from Chesapeake Bay sediments, Fig.5.1, (Bricker et al., 1977) and Long Island Sound, Fig.5.2, (Aller, 1980) are shown. MnAlk apparent solubility products are similar for both sets, ranging from 0.1 to 1.0  $\text{mM}^2$ .

#### 1. Equations and Solutions for $\text{MnCO}_3(\text{s})$ and $\text{CaCO}_3(\text{s})$

The mass balance and mass action equations for a closed system are:

Alkalinity mass balance:

$$\text{Alk}_T - 2 \text{CaAlk} - 2 \text{MnAlk} - \text{Alk}_d = 0 \quad (55)$$

Calcium mass balance:

$$\text{Ca}_T - \text{Ca}_d - \text{CaAlk} = 0 \quad (56)$$



# Chesapeake Bay Pore Water

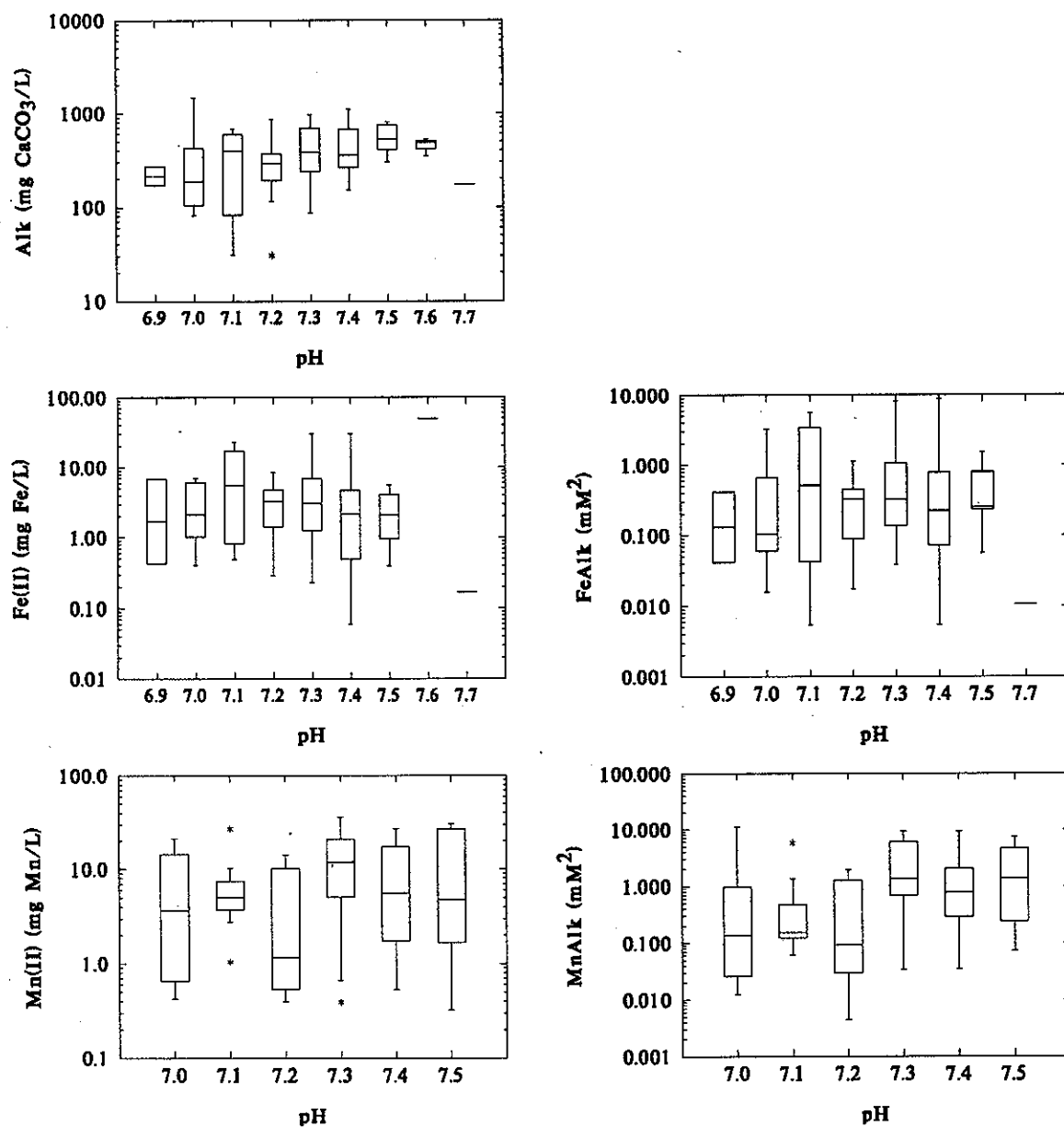


Figure 5.1

## Long Island Sound Pore Water

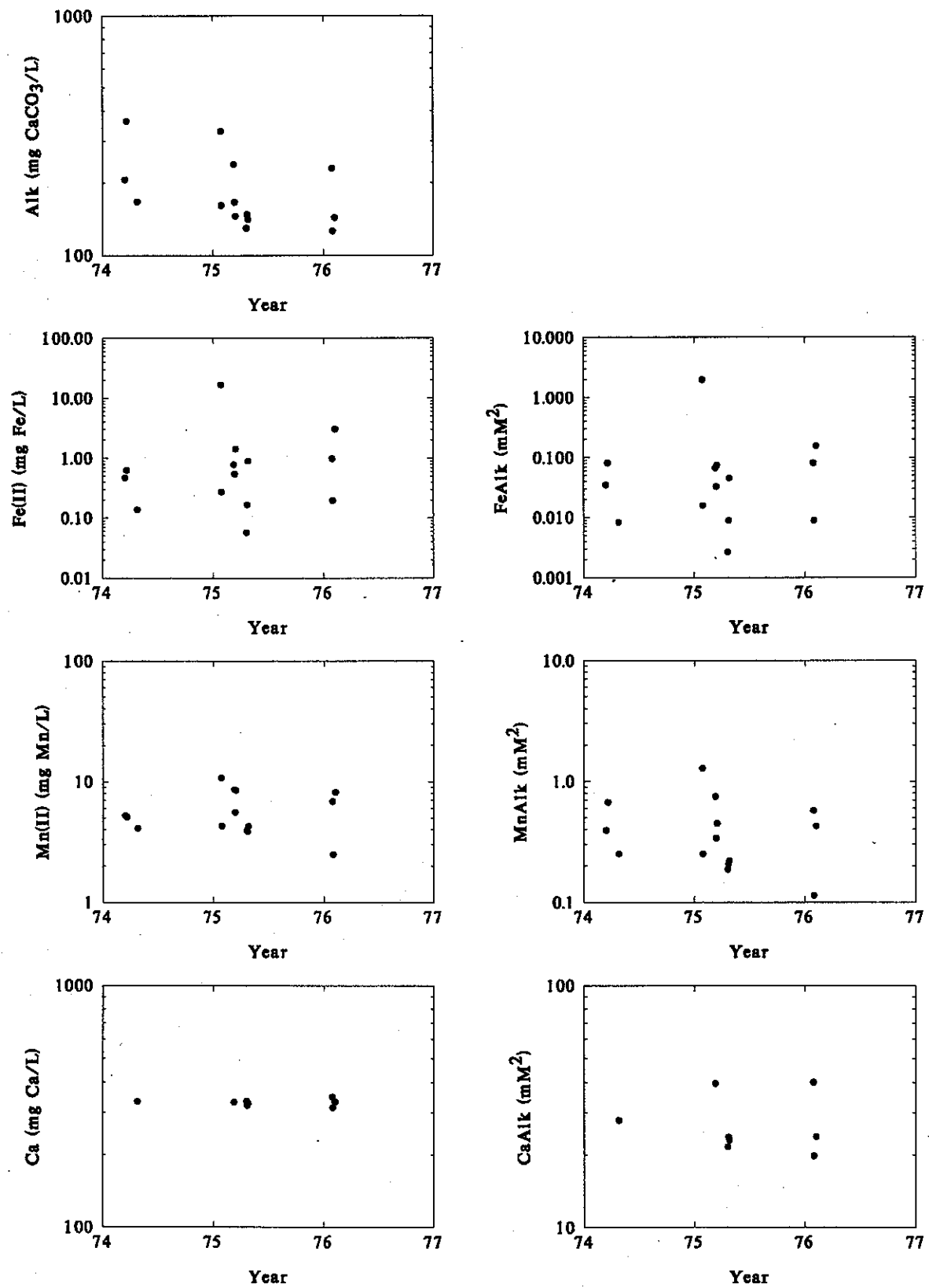


Figure 5.2

Manganese mass balance:

$$\text{Mn}_T - \text{Mn}_d - \text{MnAlk} = 0 \quad (57)$$

$\text{CaCO}_3(\text{s})$  Solubility:

$$\text{Ca}_d \text{Alk}_d = K_{\text{sp,CaAlk}} \quad (58)$$

$\text{MnCO}_3(\text{s})$  Solubility

$$\text{Mn}_d \text{Alk}_d = K_{\text{sp,MnAlk}} \quad (59)$$

where  $\text{Alk}_T$ ,  $\text{Alk}_d$  are the total and dissolved alkalinity,  $\text{Mn}_T$  and  $\text{Mn}_d$  are the total and dissolved manganese, and  $\text{Ca}_T$  and  $\text{Ca}_d$  are the total and dissolved calcium.

Eliminating all the independent variables except  $\text{MnAlk}$  yields a quadratic equation of the form:

$$a \text{MnAlk}^2 + b \text{MnAlk} + c = 0 \quad (60)$$

with coefficients:

$$a = -4 ( K_{\text{sp,MnAlk}} + K_{\text{sp,CaAlk}} ) \quad (61)$$

$$b = 2 ( 2 K_{\text{sp,MnAlk}} \text{Mn}_T + 4 K_{\text{sp,CaAlk}} \text{Mn}_T - 2 \text{Ca}_T K_{\text{sp,MnAlk}} + \text{Alk}_T K_{\text{sp,MnAlk}} ) \quad (62)$$

$$c = -2 ( 2 K_{\text{sp,CaAlk}} \text{Mn}_T^2 - 2 \text{Ca}_T K_{\text{sp,MnAlk}} \text{Mn}_T + \text{Alk}_T K_{\text{sp,MnAlk}} \text{Mn}_T - K_{\text{sp,MnAlk}}^2 ) \quad (63)$$

The equation for  $\text{CaAlk}$  is also quadratic:

$$a \text{CaAlk}^2 + b \text{CaAlk} + c = 0 \quad (64)$$

with:

$$a = 2 \quad (65)$$

$$b = (2 \text{ MnAlk} - 2 \text{ Ca}_T - \text{Alk}_T) \quad (66)$$

$$c = -2 \text{ Ca}_T \text{ MnAlk} - K_{\text{sp,CaAlk}} + \text{Alk}_T \text{ Ca}_T \quad (67)$$

It is remarkable that adding manganese as a component and  $\text{MnCO}_3(\text{s})$  as a solid phase does not materially complicate the solution. It requires only the solutions of quadratic equations.

The solution procedure is to solve the quadratic equation for MnAlk which yields two solutions. For each of these solutions, two solutions for CaAlk are found. For each of the four possible solutions the dissolved concentrations are computed. Then the solutions are checked for the following conditions. Are all concentrations positive? Are there no oversaturated solids? If both of these conditions are true, then the feasible solution has been found. If no feasible solution is found, then either CaAlk and/or MnAlk are zero and the solution is undersaturated with either or both of these solids. The equations for these cases are given in the Appendix.

## 2. Results

An example computation is presented below. The computer program that produced the results is listed in Appendix III. The calcium concentration is kept constant,  $\text{Ca} = 300 \text{ mg/L} = 7.5 \text{ mM}$  which is approximately the concentration in overlying water for the Long Island Sound sediment data. The solubility products are:  $K_{\text{sp,CaAlk}} = 10 \text{ (mM)}^2$  and  $K_{\text{sp,MnAlk}} = 0.4 \text{ (mM)}^2$ . Total alkalinity is varied from 1 to 20 mM and total manganese from 0.05 - 0.5 mM. These ranges are characteristic. Note that the alkalinity is much larger than the manganese concentrations. The tables below have alkalinity varying in the y direction and manganese in the x direction.

The computed solid phase concentrations, MnAlk and CaAlk, are:

#### MnAlk (mM)

##### Alk<sub>T</sub> (mM)

1.0000	0	0	0	0	0	0.699
1.8206	0	0	0	0	0.0309	0.2094
3.3145	0	0	0	0	0.0777	0.2566
6.0342	0	0	0	0.0389	0.1525	0.3325
10.9856	0	0.0045	0.0504	0.1230	0.2382	0.4207
20.0000	0.0198	0.0490	0.0952	0.1685	0.2847	0.4688
Mn <sub>T</sub> (mM)	0.500	0.0792	0.1256	0.1991	0.3155	0.5000

#### CaAlk (mM)

##### Alk<sub>T</sub> (mM)

1.0000	0	0	0	0	0	
1.8206	0.4101	0.4101	0.4101	0.4101	0.3844	0.2348
3.3145	1.6152	1.6152	1.6152	1.6152	1.5548	1.4146
6.0342	3.5210	3.5210	3.5210	3.4971	3.4266	3.3132
10.9856	5.6321	5.6309	5.6190	5.5998	5.5689	5.5184
20.0000	6.7445	6.7429	6.7404	6.7364	6.7299	6.7195
Mn <sub>T</sub> (mM)	0.0500	0.0792	0.1256	0.1991	0.3155	0.5000

CaAlk forms as Alk<sub>T</sub> is increased. Its concentration is not affected by the concentration of Mn<sub>T</sub>. MnAlk also forms as Alk<sub>T</sub> and Mn<sub>T</sub> are increased. Its concentration is affected by both independent variables.

## B. Sediment Model Equations and Solutions

The structure of the manganese flux model is illustrated in Fig.5.3. The oxidation of Mn(II) to MnO<sub>2</sub>(s) occurs in the aerobic layer, and the reduction of MnO<sub>2</sub>(s) to Mn(II) occurs in the anaerobic layer. The partitioning of Mn(II) in the anaerobic layer is controlled by the solubility of MnCO<sub>3</sub>(s). In order to calculate the carbonate concentration, the influence of CaCO<sub>3</sub>(s) must also be considered. Both these reactions are shown as the solubility of MnAlk and CaAlk, as discussed above.

Hence, the equations for the sediment model are a combination of the equations for the linear partitioning model for manganese, with the addition of the equations for calcium, from the calcium - alkalinity model, and a solubility equation for MnAlk. They are listed below.

### 1. Mass Balance Equations:

Layer 1 Alkalinity:

$$-s (Alk(1) - Alk(0)) + K_{L12} (Alk(2) - 2 CaAlk(2) - 2 MnAlk(2) - Alk(1)) = 0 \quad (68)$$

Layer 2 Alkalinity:

$$\begin{aligned} & -K_{L12} (Alk(2) - 2 CaAlk(2) - 2 MnAlk(2) - Alk(1)) \\ & -w_2 (2 CaAlk(2) + 2 MnAlk(2)) + J_{Alk} = 0 \end{aligned} \quad (69)$$

Layer 1 Calcium:

$$-s Ca(1) + K_{L12} (Ca(2) - CaAlk(2) - Ca(1)) + s Ca(0) = 0 \quad (70)$$

# MANGANESE FLUX MODEL

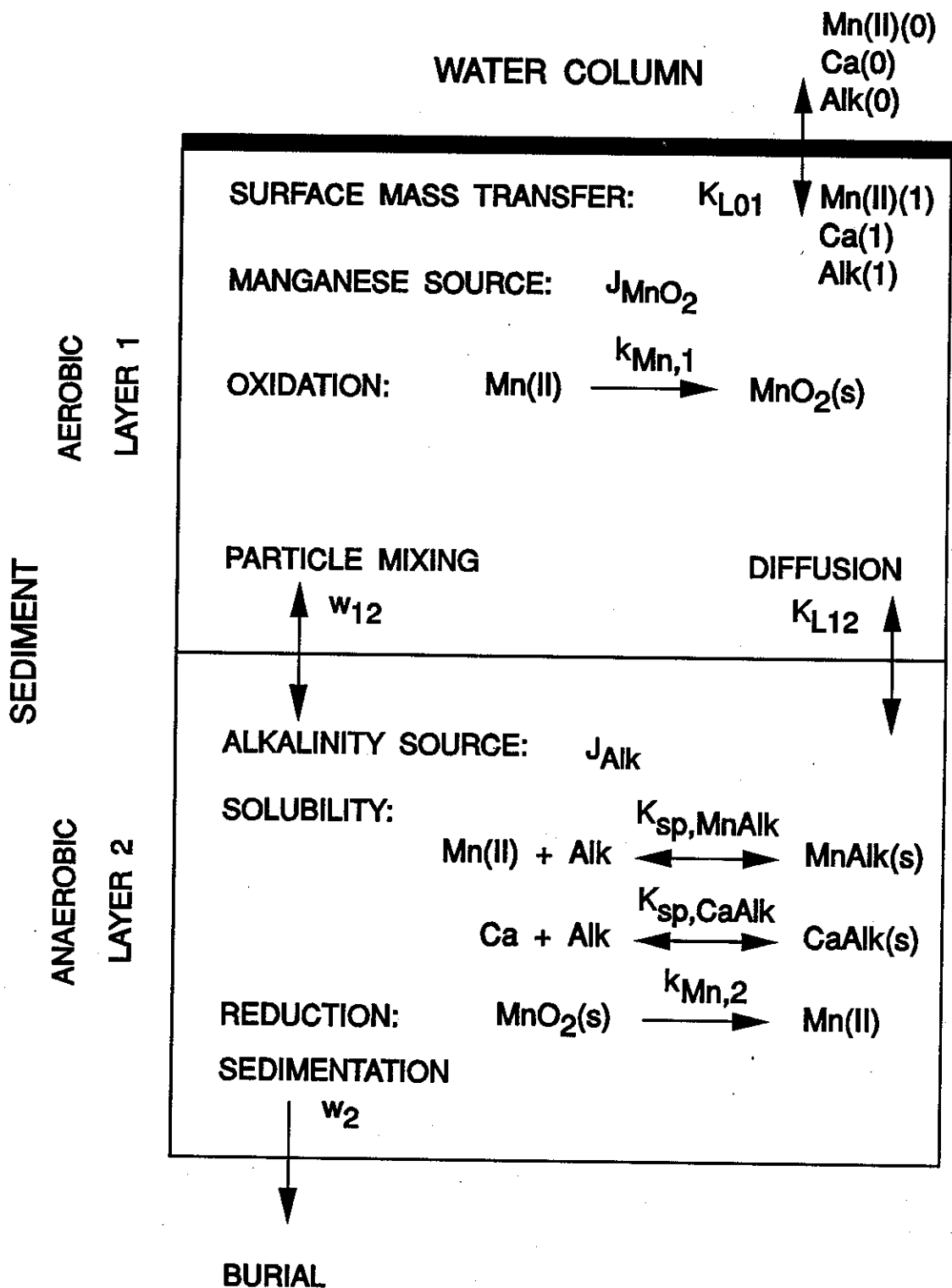


Figure 5.3

Layer 2 Calcium:

$$-K_{L12} (Ca(2) - CaAlk(2) - Ca(1)) - w_2 CaAlk(2) = 0 \quad (71)$$

Layer 1 Mn(II):

$$\begin{aligned} & (-s(f_{d1} Mn(1) - Mn(0)) + K_{L12} (Mn(2) - MnAlk(2) - f_{d1} Mn(1)) \\ & + w_{12} (f_{dis} MnAlk(2) - f_{p1} Mn(1)) - k_{Mn,1} f_{d1} Mn(1)) = 0 \end{aligned} \quad (72)$$

Layer 2 Mn(II):

$$\begin{aligned} & (-K_{L12} (Mn(2) - MnAlk(2) - f_{d1} Mn(1)) \\ & - w_{12} (f_{dis} MnAlk(2) - f_{p1} Mn(1)) - w_2 MnAlk(2) + k_{Mn,2} MnO_2(2)) = 0 \end{aligned} \quad (73)$$

Layer 1 MnO<sub>2</sub>(s):

$$k_{Mn,1} f_{d1} Mn(1) + w_{12} (MnO_2(2) - MnO_2(1)) + J_{MnO_2} = 0 \quad (74)$$

Layer 2 MnO<sub>2</sub>(s):

$$-k_{Mn,2} MnO_2(2) - w_{12} (MnO_2(2) - MnO_2(1)) - w_2 MnO_2(2) = 0 \quad (75)$$

## 2. Mass Action Equations:

Layer 2 CaCO<sub>3</sub>(s) solubility:

$$(Ca(2) - CaAlk(2)) (Alk(2) - 2 CaAlk(2) - 2 MnAlk(2)) - K_{sp,CaAlk} = 0 \quad (76)$$



Layer 2  $\text{MnCO}_3(\text{s})$  solubility:

$$(\text{Mn}(2) - \text{MnAlk}(2)) (\text{Alk}(2) - 2 \text{CaAlk}(2) - 2 \text{MnAlk}(2)) - K_{\text{sp, MnAlk}} = 0 \quad (77)$$

### 3. Solution

The first step in the solution is to solve for all the dependent variables except  $\text{CaAlk}(2)$  and  $\text{MnAlk}(2)$  using the mass balance equations. The solutions are:

$$\text{Alk}(1) = \frac{(\text{Alk}(2) K_{\text{L12}} - 2 \text{CaAlk}(2) K_{\text{L12}} - 2 K_{\text{L12}} \text{MnAlk}(2) + \text{Alk}(0) s)}{(K_{\text{L12}} + s)} \quad (78)$$

$$\text{Ca}(1) = \frac{(-( \text{CaAlk}(2) K_{\text{L12}} ) + \text{Ca}(2) K_{\text{L12}} + \text{Ca}(0) s)}{(K_{\text{L12}} + s)} \quad (79)$$

$$\text{Mn}(1) = (-K_{\text{L12}} \text{MnAlk}(2)) + K_{\text{L12}} \text{Mn}(2) + \text{Mn}(0) s$$

$$+ f_{\text{dis}} \text{MnAlk}(2) w_{12}) / (f_{\text{d1}} K_{\text{L12}} + f_{\text{d1}} k_{\text{Mn1}} + f_{\text{d1}} s + f_{\text{p1}} w_{12}) \quad (80)$$

and:

$$\begin{aligned} \text{MnO}_2(1) = & ((k_{\text{Mn}2} + w_{12} + w_2)(J_{\text{MnO}2} k_{\text{Mn}1} + J_{\text{MnO}2} s \\ & + k_{\text{Mn}1} \text{Mn}(0) s - k_{\text{Mn}1} \text{MnAlk}(2) w_2) / (w_{12}(k_{\text{Mn}2} s + k_{\text{Mn}1} w_2 + s w_2)) \end{aligned} \quad (81)$$

$$\begin{aligned} \text{MnO}_2(2) = & ((J_{\text{MnO}2} k_{\text{Mn}1} + J_{\text{MnO}2} s + k_{\text{Mn}1} \text{Mn}(0) s \\ & - k_{\text{Mn}1} \text{MnAlk}(2) w_2) / (k_{\text{Mn}2} s + k_{\text{Mn}1} w_2 + s w_2) \end{aligned} \quad (82)$$

It is the layer two solutions that are needed for the mass action equations. These are written in the following form in order to substitute for various parameter groups and to isolate the dependency on CaAlk and MnAlk:

$$\text{Alk}(2) = \text{ja}0 + \text{jac} \text{CaAlk}(2) + \text{jam} \text{MnAlk}(2) \quad (83)$$

$$\text{Ca}(2) = \text{jc}0 + \text{jcc} \text{CaAlk}(2) + \text{jcm} \text{MnAlk}(2) \quad (84)$$

$$\text{Mn}(2) = \text{jm}0 + \text{jmc} \text{CaAlk}(2) + \text{jmm} \text{MnAlk}(2) \quad (85)$$

where the notation denotes the jacobian (j) of the equation (a,c,m for Alk, Ca, Mn) with respect to nothing, (0, the constant term) or the variables (c, m for CaAlk, MnAlk).

The jacobians for alkalinity are:

$$ja0 = Alk(0) + jalk / Kl12 + jalk / s \quad (86)$$

$$jac = 2 - 2 w_2 / K_{L12} - 2 w_2 / s \quad (87)$$

$$jam = 2 - 2 w_2 / K_{L12} - 2 w_2 / s \quad (88)$$

For calcium they are:

$$jc0 = Ca(0) \quad (89)$$

$$jcc = 1 - w_2 / Kl12 - w_2 / s \quad (90)$$

$$jcm = 0 \quad (91)$$

and for manganese they are:

$$\begin{aligned}
 j_{m0} = & ((f_{d1} J_{MnO2} K_{L12} k_{Mn2} + f_{d1} J_{MnO2} k_{Mn2} \\
 & + f_{d1} J_{MnO2} k_{Mn2} s + f_{d1} K_{L12} k_{Mn2} Mn(0) s \\
 & + f_{d1} k_{Mn1} k_{Mn2} Mn(0) s + f_{p1} J_{MnO2} k_{Mn2} w_{12} \\
 & f_{p1} k_{Mn2} Mn(0) s w_{12} + f_{d1} K_{L12} Mn(0) s w_2 + f_{p1} Mn(0) s w_{12} w_2) \\
 & / (f_{d1} K_{L12} (k_{Mn2} s + k_{Mn1} w_2 + s w_2))
 \end{aligned} \tag{92}$$

$$j_{mc} = 0 \tag{93}$$

$$\begin{aligned}
 j_{mm} = & ((f_{d1} K_{L12} k_{Mn2} s - f_{dis} f_{d1} k_{Mn2} s w_{12} + f_{d1} K_{L12} k_{Mn1} w_2 - f_{d1} K_{L12} k_{Mn2} w_2 \\
 & - f_{d1} k_{Mn1} k_{Mn2} w_2 + f_{d1} K_{L12} s w_2 - f_{d1} k_{Mn2} s w_2 - f_{dis} f_{d1} k_{Mn1} w_{12} w_2 \\
 & - f_{dis} f_{d1} s w_{12} w_2 - f_{d1} K_{L12} w_2^2 - f_{d1} k_{Mn1} w_2^2 - f_{d1} s w_2^2 - f_{p1} w_{12} w_2^2)
 \end{aligned}$$

$$/ (f_{d1} K_{L12} (k_{Mn2} s + k_{Mn1} w_2 + s w_2))) \quad (94)$$

An important relationship among these coefficients is:

$$jac = 2 jcc \quad (95)$$

$$jam = 2 jcc \quad (96)$$

Using these equations and substituting into the mass action equations yields quadratic equations for both CaAlk and MnAlk. The form is:

$$a \text{CaAlk}^2 + b \text{CaAlk} + c = 0 \quad (97)$$

and similarly for MnAlk. The coefficients for MnAlk(2) are denoted by the subscript Mn:

$$\begin{aligned} a_{Mn} = & 2 k_{spCaAlk} + 2 jmm^2 k_{spCaAlk} + jmm (-4 k_{spCaAlk} - 2 k_{spMnAlk}) \\ & + 2 k_{spMnAlk} + jcc (-2 k_{spMnAlk} + 2 jmm k_{spMnAlk}) \end{aligned} \quad (98)$$

$$\begin{aligned} b_{Mn} = & jm0 (-4 k_{CaAlk} + 4 jmm k_{CaAlk} - 2 k_{MnAlk}) \\ & + jc0 (2 k_{MnAlk} - 2 jmm k_{MnAlk}) + ja0 (-k_{MnAlk} + jmm k_{MnAlk}) \end{aligned} \quad (99)$$

$$c_{Mn} = -(-2jm0^2 k_{CaAlk} + k_{MnAlk}^2 + jm0(-ja0 k_{MnAlk} + 2jc0 k_{MnAlk})) \quad (100)$$

and for CaAlk(2) which are denoted by the subscript Ca:

$$a_{Ca} = 2 - 4jcc + 2jcc^2 \quad (101)$$

$$b_{Ca} = ja0(-1 + jcc) + (-2 + 2jcc)jc0 + 2MnAlk(2) - 4jccMnAlk(2) + 2jcc^2MnAlk(2) \quad (102)$$

$$c_{Ca} = -(-ja0jc0 + k_{CaAlk} + jc0(2MnAlk(2) - 2jccMnAlk(2))) \quad (103)$$

The solution procedure is to solve the quadratic equation for MnAlk(2) which yields two solutions. For each of these solutions, two solutions for CaAlk(2) are found. For each of the four possible solutions the rest of the variables are computed. Then the solutions are checked for the following conditions. Are all concentrations positive? Are there no oversaturated solids? If both of these conditions are true, then the feasible solution has been found. If no feasible solution is found, then either CaAlk and/or MnAlk are zero and the solution is undersaturated with either or both of these solids.

Once again, the solutions are found from the roots of quadratic equations. They are very similar to the batch reactor equations, although the coefficients of the equations are much more involved. Nevertheless, no essential complexity is introduced and the numerical solutions are straightforward.

### C. Results

A preliminary calibration to the Long Island Sound data is shown in Fig.5.4. The additional parameter values are presented in Table 3 and the computer program that produced the results is listed in Appendix IV.

Table 3

Parameter Values for the  $\text{MnCO}_3$  and  $\text{CaCO}_3$  Model

$k_{\text{Mn},1}$	0.03	m/d
$k_{\text{Mn},2}$	10	m/d
$\pi_1$	300	L/kg
$K_{\text{sp},\text{CaCO}_3}$	20	$\text{mM}^2$
$K_{\text{sp},\text{MnCO}_3}$	0.5	$\text{mM}^2$

The observed pore water alkalinity, calcium, and  $\text{CaCO}_3(\text{s})$  are reproduced by the model calculations. The data are plotted at  $J[\text{NH}_4] = 10 \text{ mg/m}^2\text{-d}$  for convenience. The fit is actually slightly better than the model for  $\text{CaCO}_3(\text{s})$  alone, Fig.4.3.

The manganese results are shown in Fig.5.5. Pore water manganese is reproduced reasonably closely (C) while the computed concentration of  $\text{MnCO}_3(\text{s})$  is higher than the observation (D). The manganese flux variation with respect to ammonia flux (A,B) is more pronounced than the linear partitioning model, Fig.3.3. However it is still not as pronounced as the observations (E).

#### D. Conclusions

# Manganese - Calcium - Alkalinity Model

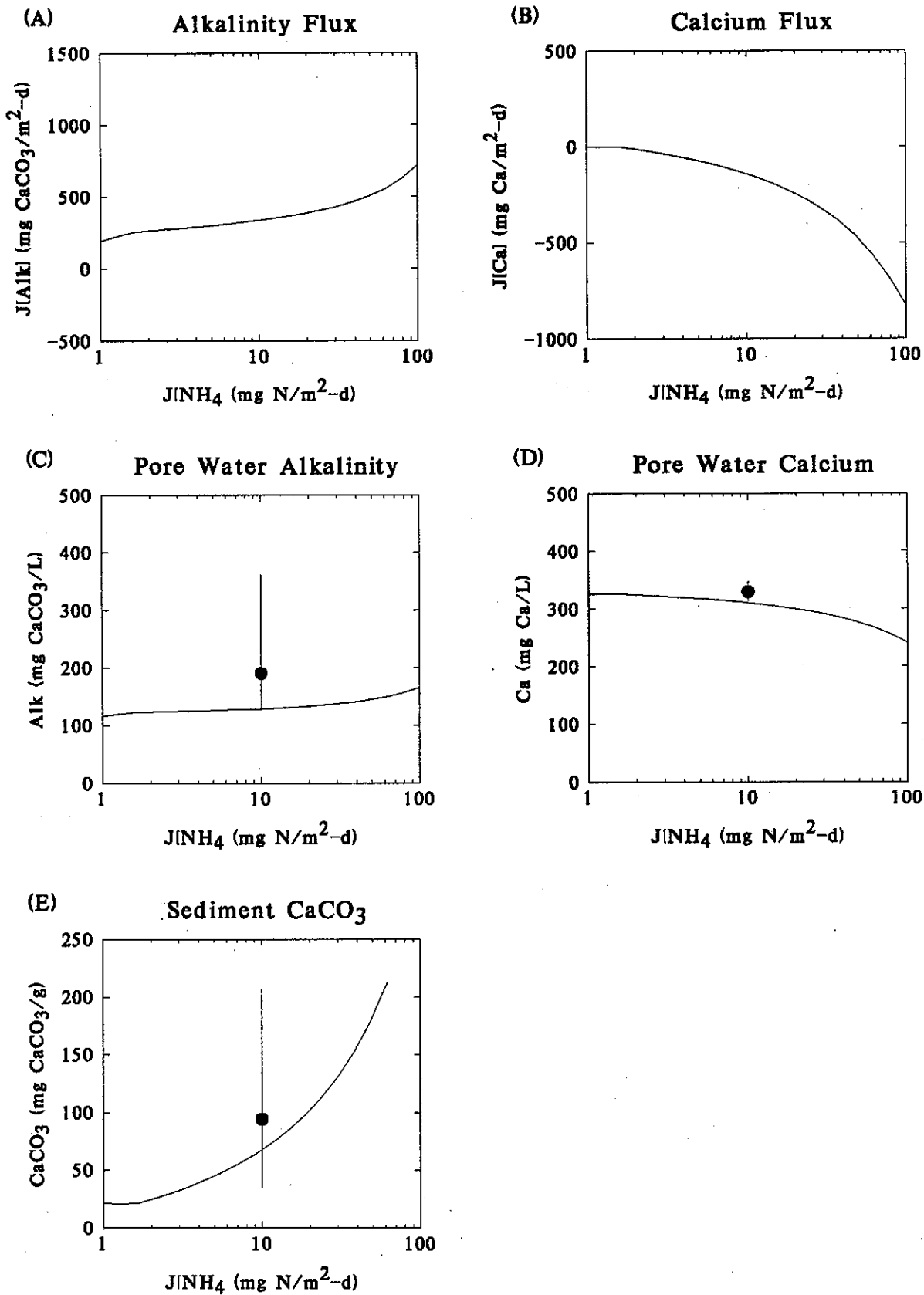


Figure 5.4



# Manganese - Calcium - Alkalinity Model

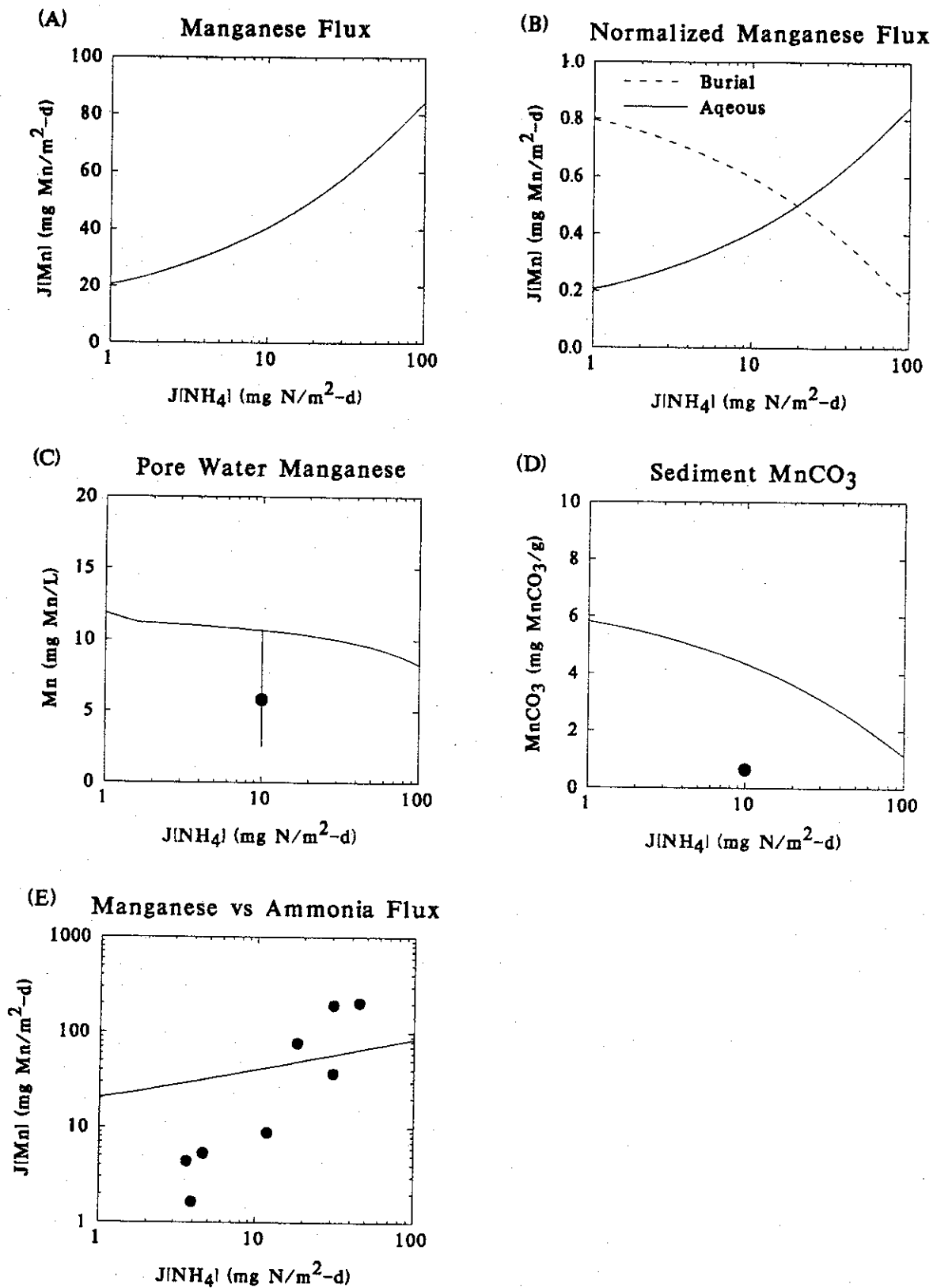


Figure 5.5

The inclusion of carbonate solubility controls for manganese partitioning in the anaerobic layer has slightly improved the model results. However, there is still a substantial variation of  $J[\text{Mn}]$  with respect to  $J[\text{NH}_4]$  that is unexplained. Perhaps it is a time variable effect. This possibility is examined in the next section.

## VI. Application to MERL Data

### A. Review of MERL Data

The MERL mesocosms are large outdoor tanks approximately 1.8 meters in diameter and have a water depth of 5.0 meters. Narragansett Bay water flows through at a rate to establish a detention time of approximately 30 days. The tanks have a mixer to control stratification. Sediments are obtained using a large box core which maintains the vertical orientation and the top 40 cm are placed into containers in the bottom of the tanks (Nixon et al., 1986).

The data to be analyzed below comes from the Nutrient Addition Experiment. Its purpose was to examine the consequences of nutrient enrichment to coastal estuaries. The duration was approximately 2 1/4 years over three calendar years. The nutrient dosing was increased in a geometric series, 1X, 2X, 4X, 8X, 16X, and 32X, in addition to three control tanks. The nutrients added were inorganic nitrogen, phosphorus, and silica in a molar ratio of 12.8 N : 1.0 P : 0.91 Si to match the stoichiometry of sewage entering the bay (Nixon et al., 1986). Areal loading rates of total nitrogen to the tanks varied from 23 mg N/m<sup>2</sup>-d for the controls, 63 mg N/m<sup>2</sup>-d for 1X, 103 mg N/m<sup>2</sup>-d for 2X and so on geometrically to 1308 mg N/m<sup>2</sup>-d for the 32X (Kelly et al., 1985). As a result, mean annual water column DIN increased from 56 to 4200 ug N/L; mean annual Chla ranged from 4 to 70 ug/L, and total system carbon production ranged from 0.55 to 2.2 g C/m<sup>2</sup>-d (Nixon et al., 1986). Note that the areal loading rate increased approximately 57 fold, the DIN concentration by approximately the same ratio (75), whereas the chlorophyll a increased by only 17 fold and the total system carbon production increased by only 4 fold.

Sediment processes were also examined during the experiment. Sediment oxygen and nutrient fluxes, pore water and solid phase concentrations were also measured. In addition, manganese flux and sediment compositional data were also collected (Hunt and Kelly, 1988). These data are examined below.

## B. Application of the Nutrient Flux Model

The stand alone version of the Chesapeake Bay Sediment Model was applied to the MERL sediment data. In the stand alone version of the model, the average annual depositional flux of particulate organic nitrogen to the sediment,  $J_{PON}$ , is specified externally. Values are chosen to fit the measured ammonia fluxes. No kinetic or transport parameter values were changed initially. The required depositional fluxes are shown in Fig.6.1. Fluxes vary from less than 50 to 130 mg N/m<sup>2</sup>-d, less than a 3 fold variation.

The model is run as follows. The sediments are initially equilibrated using the depositional flux that characterizes the controls during the experiment. That is, it is assumed that the state of the sediments in the year when they were collected were similar to that in the subsequent years as indicated by the fluxes in the control mesocosms. Thus, initially all the sediments have the same concentrations as the controls. The differences occur due to the increased loading during the experiment.

The resulting ammonia fluxes are shown in Fig.6.2. The seasonal variation is reasonably well reproduced except for 32X. However, the negative fluxes in the winter, which increase as loading increases, are not captured.

The oxygen fluxes are shown in Fig.6.3. The results are remarkably good. The absolute magnitudes and the seasonal variations are reproduced up to 32X. Since the manganese model requires the surface mass transfer coefficient:  $s = SOD/O_2(0)$ , it is important that the oxygen flux be well reproduced by the model.

## C. Application of the Manganese Linear Partitioning Model

The linear partitioning model is described in Chapter III. A time variable version of the model has been implemented which utilizes the same equations as the steady state model. The same implicit integration technique is used for manganese as for the nutrients. It requires the solution of four simultaneous linear equations instead of the two for the other

## Nitrogen Depositional Flux

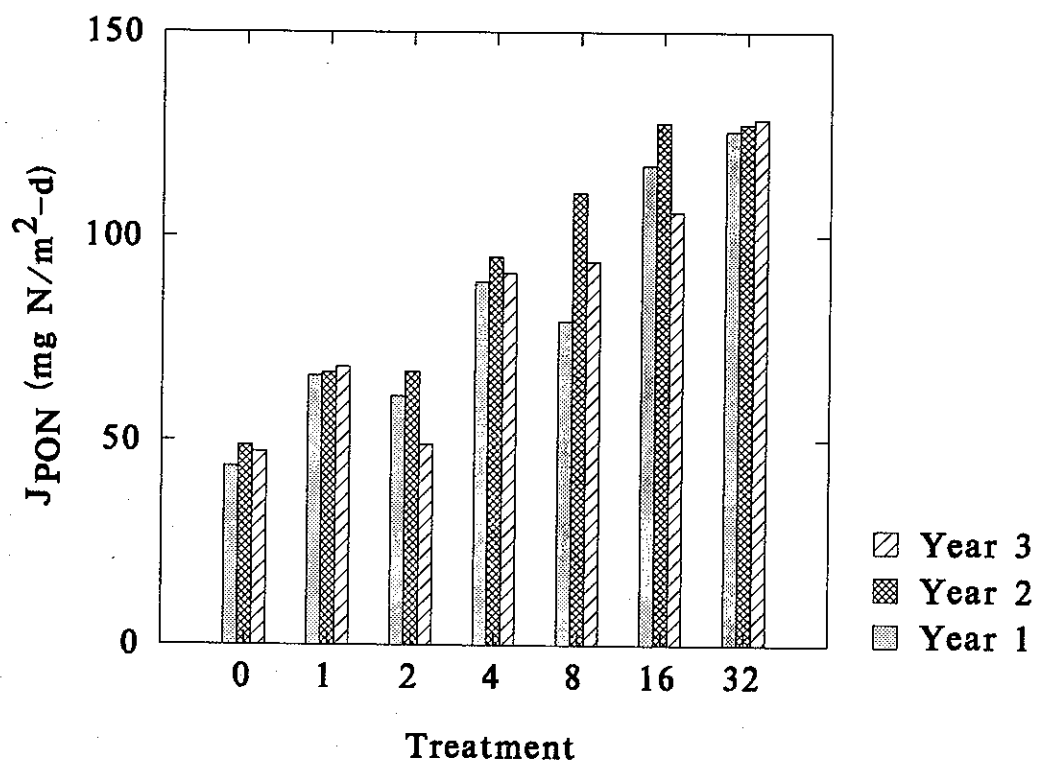


Figure 6.1

# Ammonia Flux

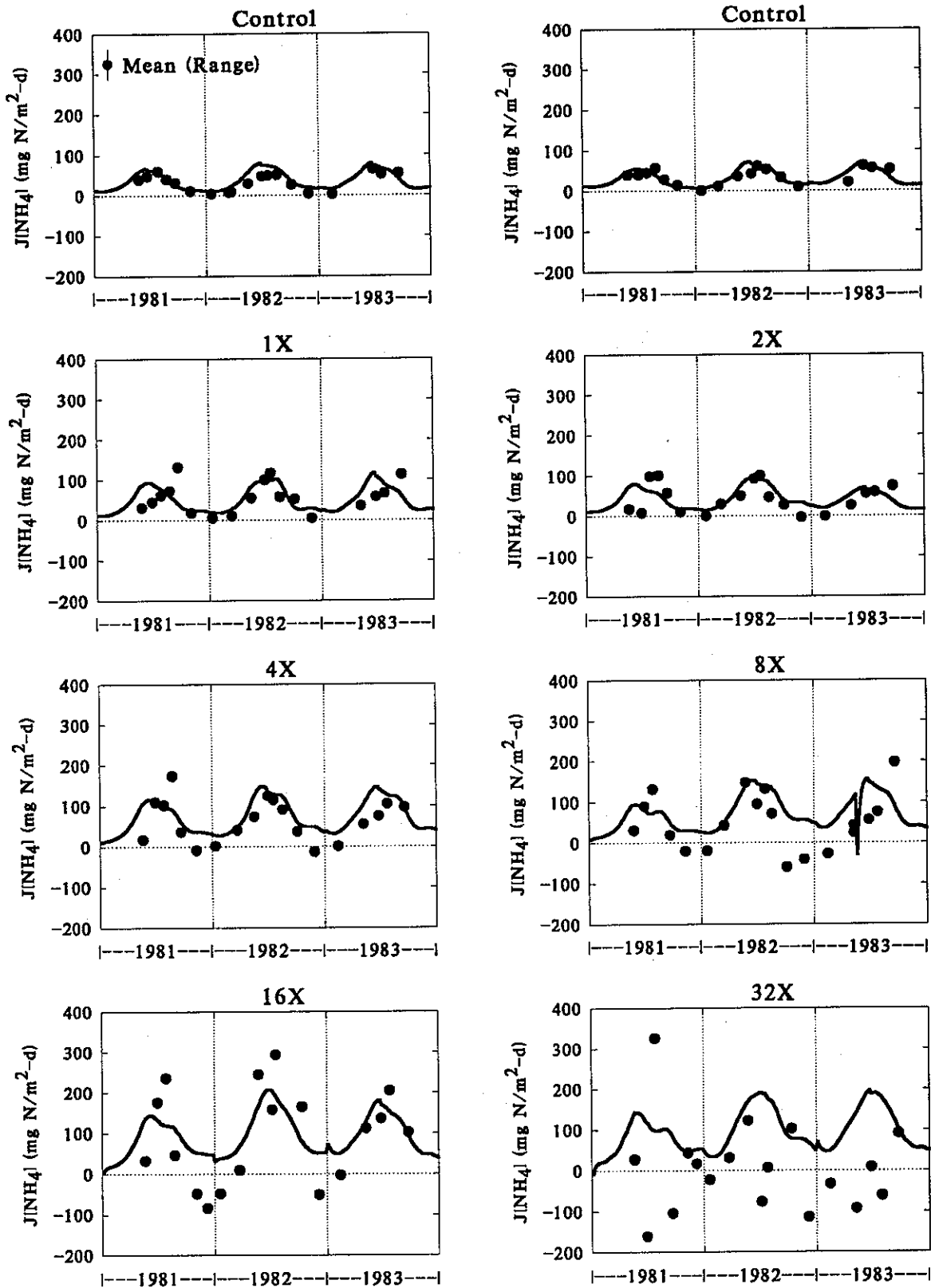


Figure 6.2

# Oxygen Flux

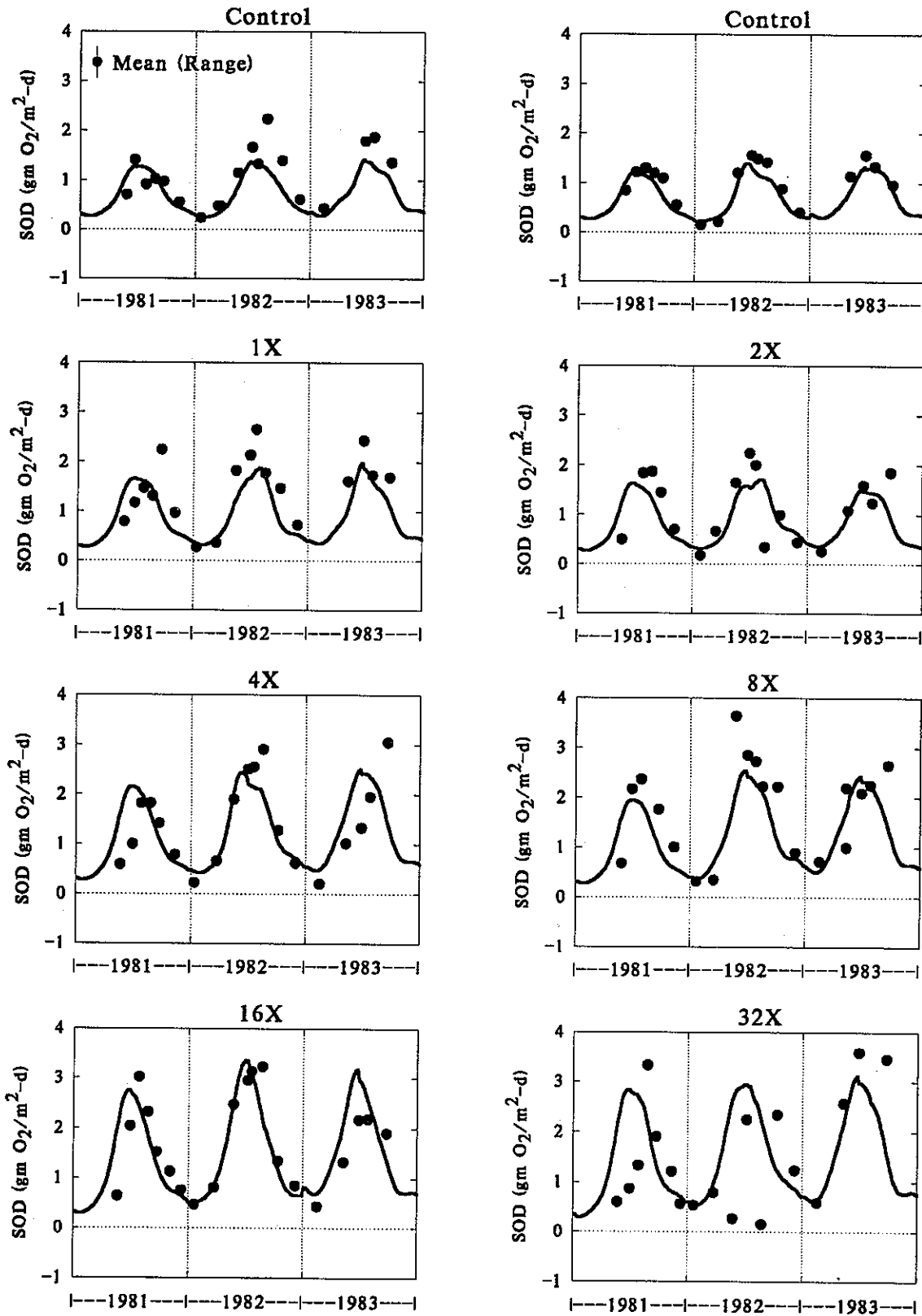


Figure 6.3

variables, since the equations for  $\text{Mn(II)}$  and  $\text{MnO}_2(\text{s})$  are coupled. This presents no difficulty, however, and the implementation is straightforward.

The model is run as follows. The nutrient portion is run as described above. For manganese, the sediments are initially equilibrated using a constant depositional flux. Then this flux is continued throughout the three years of the experiment. Thus, it is assumed that water column processes during the experiment do not change the depositional flux of manganese to the sediment. This is only an approximation since the overlying water concentrations vary as dosing varies. Fig.6.4 presents averaged seasonal data. The more highly dosed tanks usually have larger concentrations than the controls with the exception of 32X. This is most apparent in the earlier period of the experiment. However, overall the variation is not too large so that the assumption of a constant flux from the overlying water appears to be a reasonable first approximation.

A comparison of the model and observed fluxes is shown in Fig.6.5. The model is incapable of producing the strong seasonal variations in fluxes that are observed, especially at the higher loading rates. This is consistent with the findings of the steady state model. This is clearly illustrated in Fig.6.6 which compares the observed relationship between observed (left hand side) and modeled (right hand side) manganese flux and various other variables. The relationship to ammonia flux (bottom) demonstrates that the model does not reproduce the magnitude of the variation that is observed.

The pore water and solid phase concentrations are compared in Fig.6.7. The pore water concentrations are reproduced quite nicely. The sediment concentrations are approximated by the minimum annual concentrations. Since the model generates an increasing manganese flux as the dosing increases it calculates a larger loss of sediment manganese for the more highly dosed tanks. The reason this occurs is that the higher dosed tanks have a larger SOD and, therefore, a larger mass transfer coefficient and thinner aerobic layer. Thus less  $\text{Mn(II)}$  is oxidized and more escapes from the sediment. Since the quantity that is being deposited is constant across the dosing gradient, the higher dosed tanks lose more manganese. However the calculated effect is not as large as is



# Overlying Water Manganese Concentrations

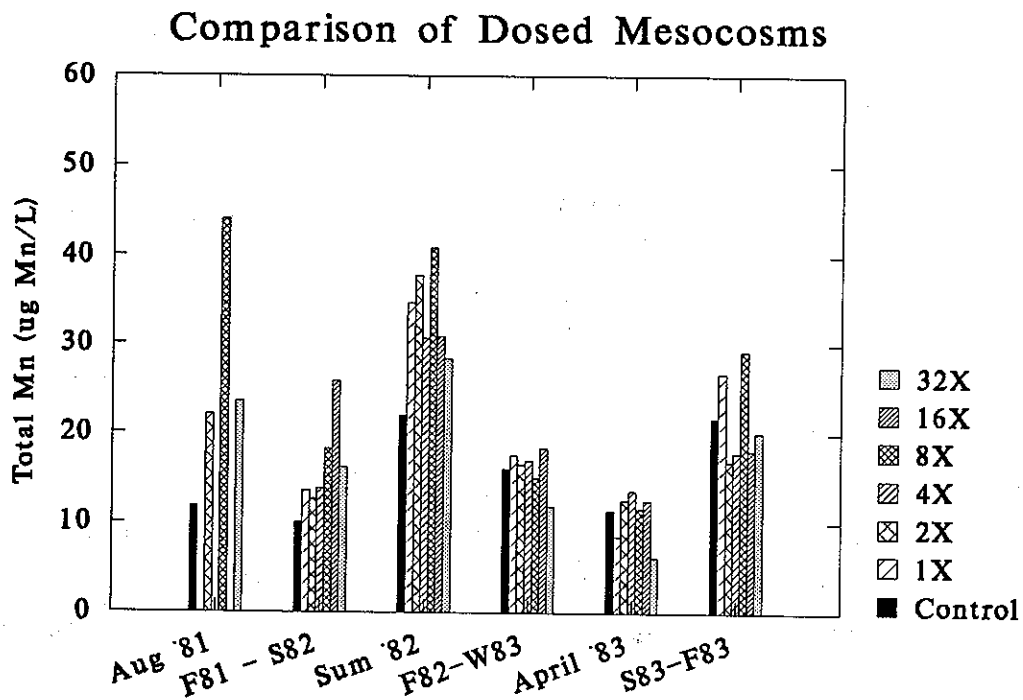
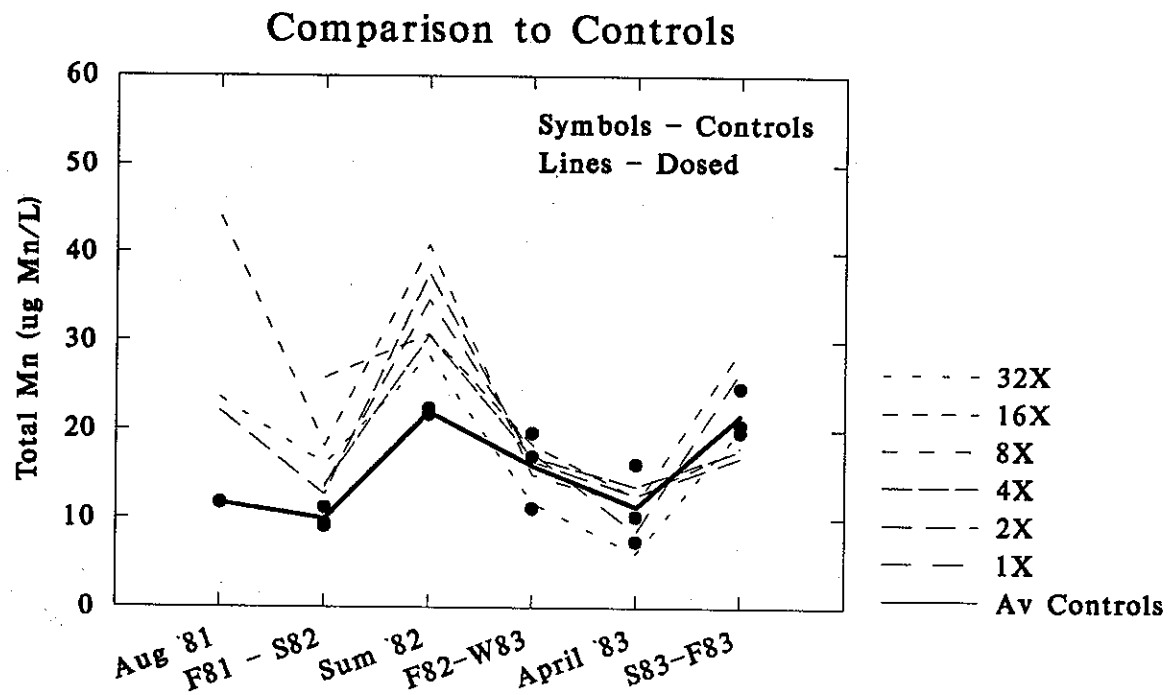


Figure 6.4

# Manganese Flux

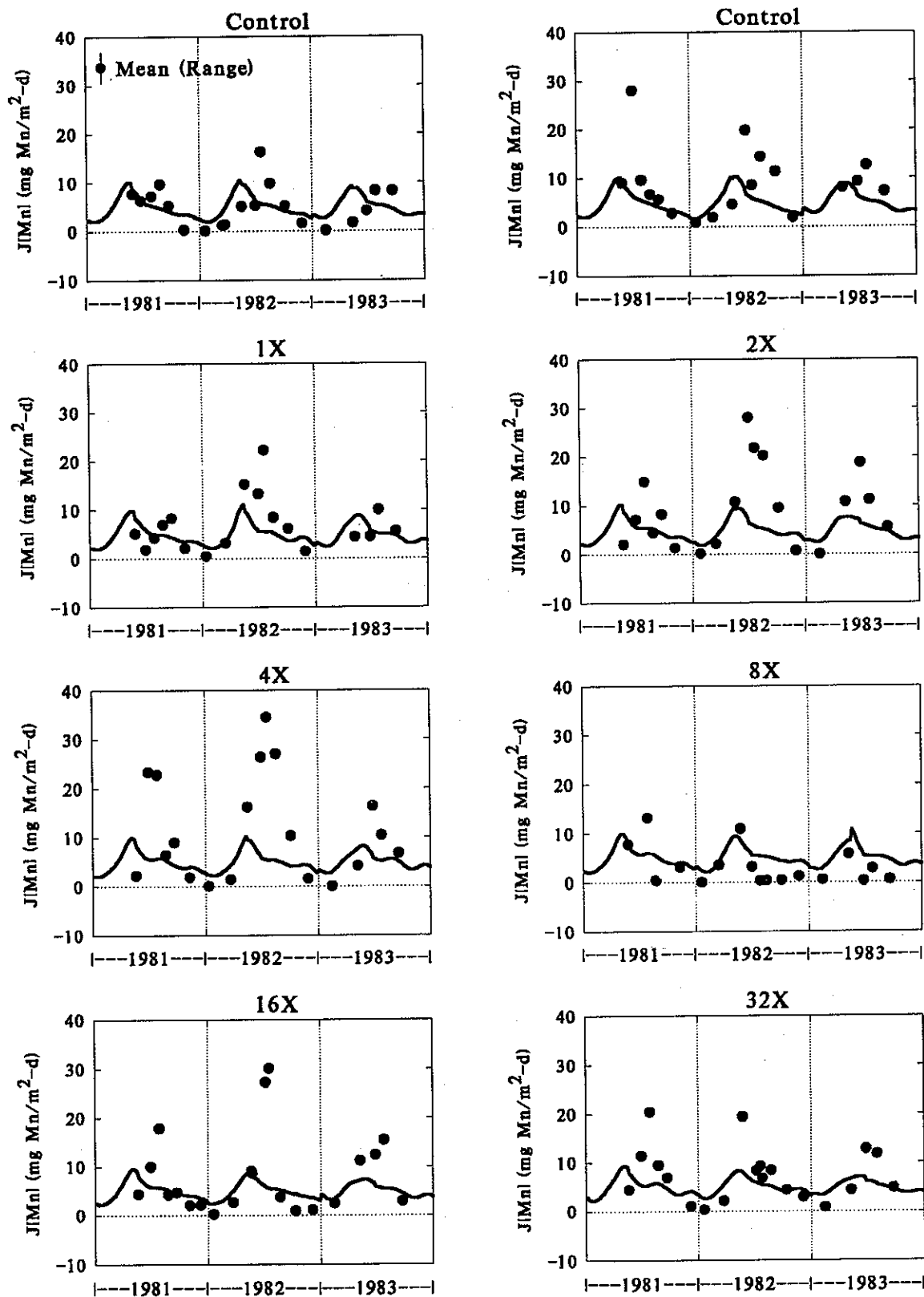


Figure 6.5

# Manganese Flux

- 0-4X
- 8X-32X

Observed

Modeled

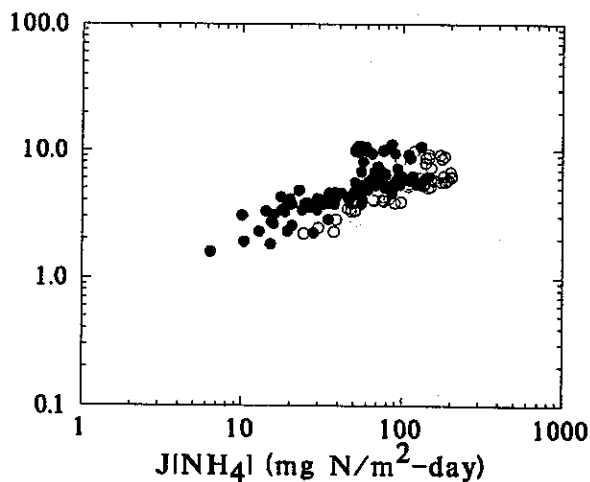
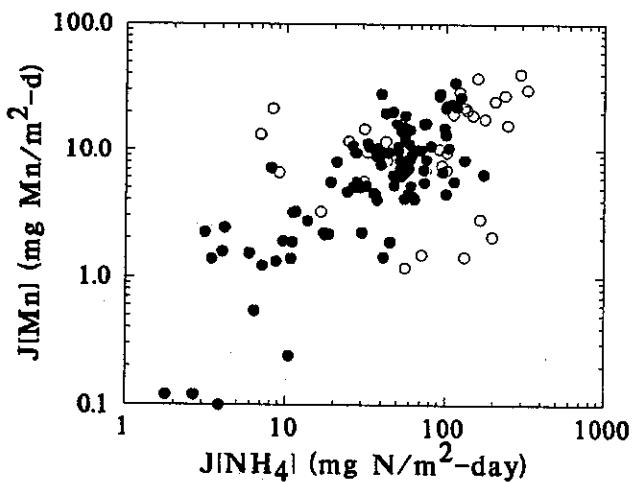
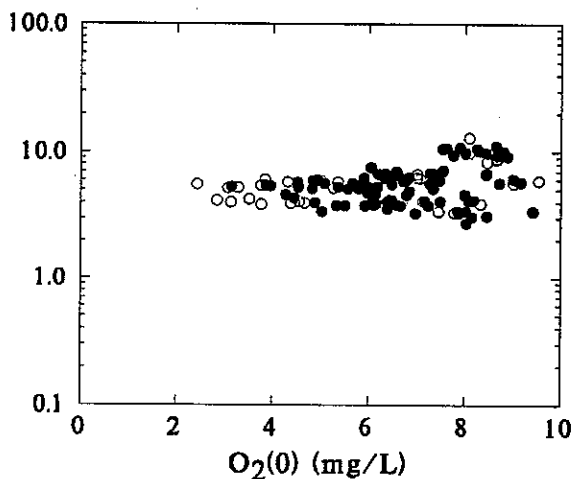
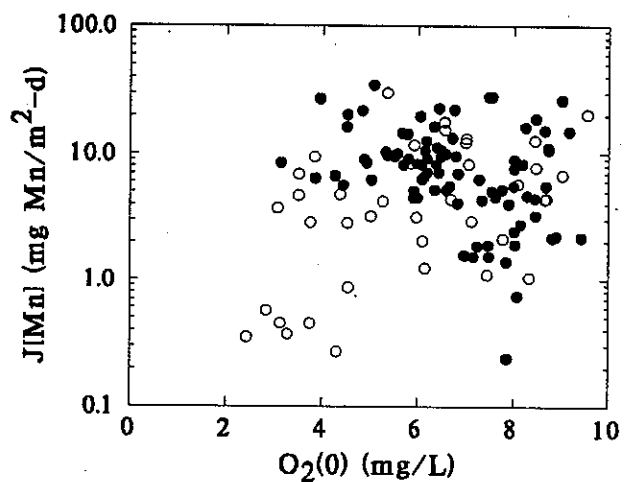
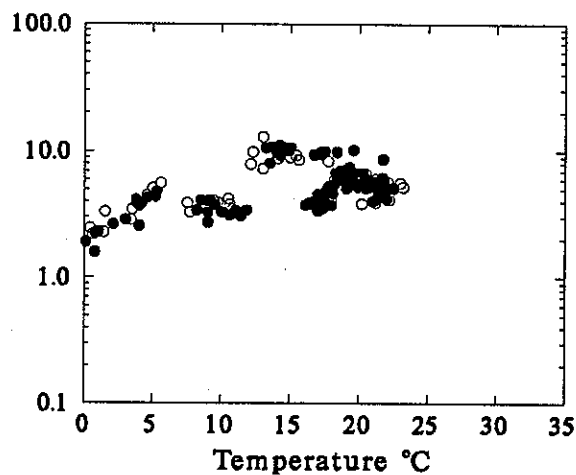
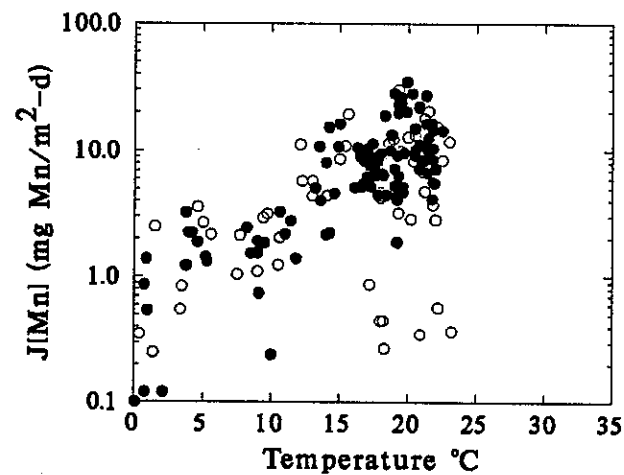


Figure 6.6

## Sediment Manganese – Particulate and Dissolved Phases

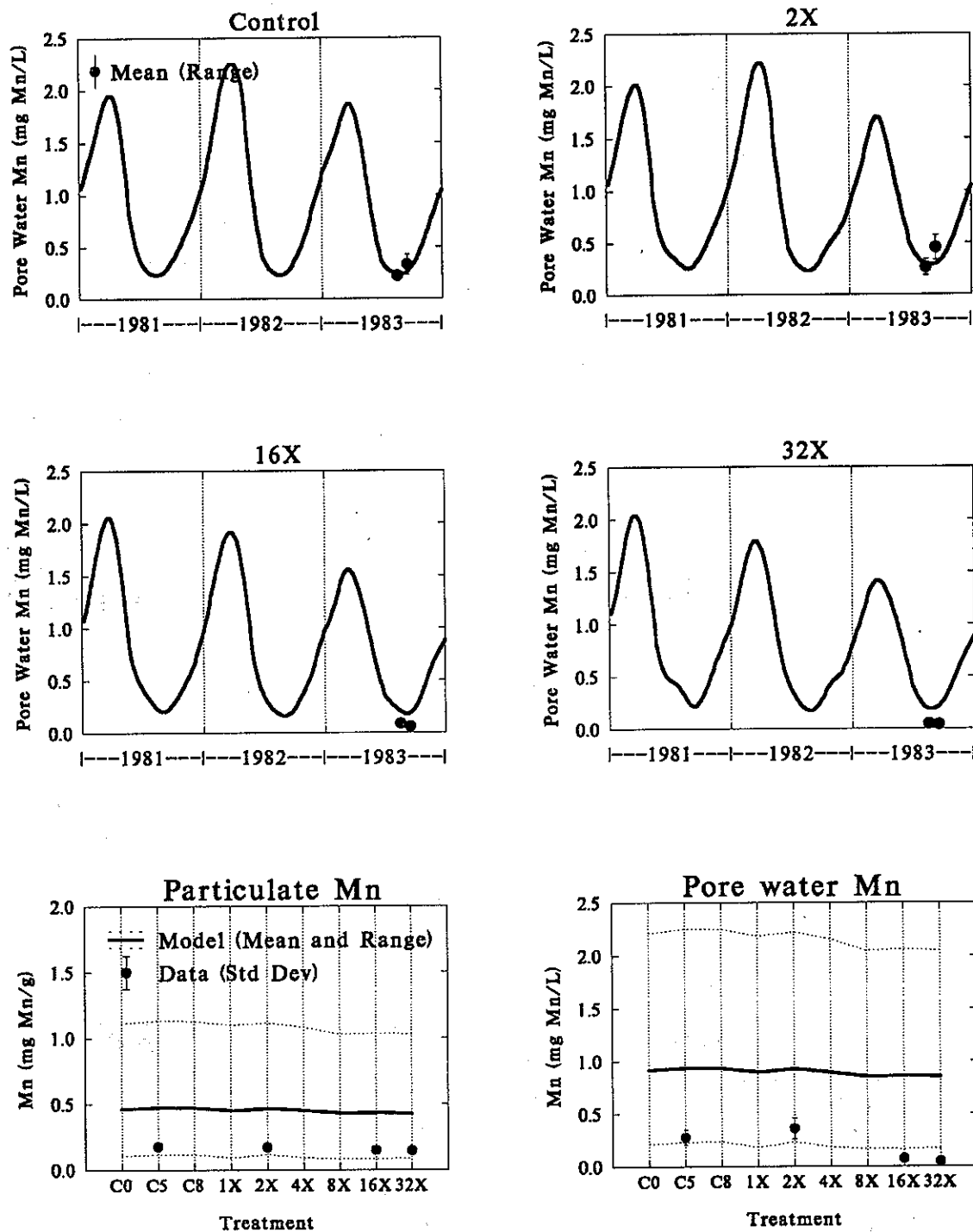


Figure 6.7

observed since the model cannot reproduce the magnitude of the variation that is observed between increased loading and manganese fluxes.

The strong relationship between manganese and ammonia flux is striking because ammonia is generated by the decomposition of organic matter, whereas manganese is not. How, then, does this strong covariation come about? The model already accounts for the variations that would be expected from the varying thickness of the aerobic layer. There must be another mechanism that is somehow related to diagenesis.

Consider the following possibility. As diagenesis occurs organic matter decomposes and the pH of pore water drops. The extent depends on the exactly which reactions are assumed to occur. A drop in pH corresponds to an increase in the solubility of MnAlk, see eq.(54). This would cause less manganese to be buried and more to escape. It is not known whether this mechanism can explain the observed seasonal variations. However, it appears to be the next logical step in the development of the manganese flux model.

#### **D. Conclusions and Recommendations**

At the present stage of model development, the manganese model captures some of the features of the data sets examined. However, it is incapable of reproducing the magnitude of the seasonal variation of manganese fluxes. This is true whether it is examined as a function of ammonia flux, as in the Long Island Sound data, or as a time series, as in the MERL data. Since the model incorporates changing thickness of the aerobic layer, which is the usual explanation of the seasonal variation, there must be another mechanism operating. The next step in the model development is to implement the mechanism that affect manganese carbonate solubility - decreasing pH with increasing diagenesis - in order to reproduce the observed seasonal variation.

## VII. References

- Aller, R.C. (1980). Diagenetic processes near the sediment-water interface of Long Island Sound. I. Decomposition and Nutrient Element Geochemistry (S, N, P). Estuarine Physics and Chemistry: Studies in Long Island Sound. Advances in Geophysics. New York, Academic Press. pp. 237-350.
- Aller, R.C. (1980). Diagenetic processes near the sediment-water interface of Long Island Sound. II. Fe and Mn. Estuarine Physics and Chemistry: Studies in Long Island Sound. Advances in Geophysics. New York, Academic Press. pp. 351-415.
- Bricker, O.P., Matisoff, G. and Holdren, G.R. (1977). Interstitial water chemistry of Chesapeake Bay sediments. Basic Data Report No.9. Maryland Geological Survey.
- Cerco, C.F. and Cole, T. (1992). Application of the Three Dimensional Eutrophication Model CE-QUAL-ICM to Chesapeake Bay. Waterways Experiment Station, U.S. Corp of Engineers. Vicksburg, MI,
- Di Toro, D.M. (1976). Combining chemical equilibrium and phytoplankton models - a general methodology. Modeling Biochemical Processes in Aquatic Ecosystems. Ann Arbor, Mich., Ann Arbor Science Press. pp. 233 - 256.
- Di Toro, D.M. and Fitzpatrick, J.F. (1993). Chesapeake Bay Sediment Flux Model. HydroQual, Inc. Mahwah, NJ.
- Hunt, C.D. and Kelly, J.R. (1988). Manganese Cycling in Coastal Regions: Response to Eutrophication. Est. Coast. and Shelf Sci. 26: pp. 527-558.
- Jaquet, J.M., Nembrini, G., Garcia, P. and Vernet, J. (1982). The manganese cycle in Lac Leman, Switzerland: The role of Metallogenium. Hydrobiol. 91: pp. 323-340.

- Jenne, E. A. (1968). Controls on Mn, Fe, Co, Ni, Cu, and Zn concentration in soils and water: The significant role of hydrous Mn and Fe oxides. In R. A. Baker (Eds.), Trace Inorganics in Water, Adv. Chem. Ser. 73. American Chemical Society Washington DC: .
- Kelly, J.R., Berounsky, V.M., Nixon, S.W. and Oviatt, C.A. (1985). Benthic-pelagic coupling and nutrient cycling across and experimental eutrophication gradient. Marine Ecology Progress Series 26: pp. 207-219.
- Morgan, J.J. (1967). Chemical equilibria and kinetic properties of manganese in natural water. In S.D. Faust, and J.V. Hunter (Eds). Principles and Applications of Water Chemistry. J. Wiley. New York
- Morel, F.M.M. (1983). Principles of Aquatic Chemistry. New York, N.Y., J. Wiley & Sons.
- Nixon, S.W., Oviatt, C.A., Frithsen, J. and Sullivan, B. (1986). Nutrients and the Productivity of Estuarine and Coastal Marine Ecosystems. J. Limnol. Soc. Sth. Afr. 12(1/2): pp. 43-71.
- Stumm, W., & Morgan, J. J. (1970). Aquatic Chemistry. New York: J. Wiley & Sons.
- Sundby, B. and Silverberg, N. (1985). Manganese fluxes in the benthic boundary layer. Limnol. Oceanogr. 30(2): pp. 372-381.
- Sundby, D., Anderson, L.G., Hall, P.O.J., Iverfeldt, A., Rutgers, L., Michiel, M. and Westerlund, S.F.G. (1986). The effect of oxygen on release and uptake of cobalt, manganese, iron and phosphate at the sediment-water interface. Geochim. Cosmochim. Acta 50(6): pp. 1281-1288.

# APPENDIX I Partitioning Model of Manganese Flux

```

A. MMANAL2.M
echo off
clear
diary mmanal2.1
format short e
format compact
echo on
% mmanal2.m - Analytical version of Mn model - Includes MnO2.
% Computes fluxes as a function of jnh4
% Define the constants
m1 = 1; m2 = 1;
kl12 = 1e-2; w12 = 1.2e-3;
w2 = 0.4/365/100;
pi1m = 100; pi2m = 100;
kmo21 = 0.1; kmo22 = 10.0 % m/d
knh41 = 0.15; %m/d
ao2n = 2.5e-5.68;
jmnin = 30; %ng/m2-d
jnh4inp = [1 2 5 10 20 50 100]; %ng/m2-d
echo off

% Convert to g/m2-d
jmnin = jmnin/1000;

% output storage
nflux = zeros(length(jnh4inp), 2);
fflux = zeros(length(jnh4inp), 2);
jnh4 = zeros(length(jnh4inp), 1);
snp = zeros(length(jnh4inp), 1);
mnconc = zeros(length(jnh4inp), 2);
mnconcp = zeros(length(jnh4inp), 4);
nfluxapprx = zeros(length(jnh4inp), 1);

disp(' Numerical and Analytical Solutions');

% jnh4 loop
for is=1:length(jnh4inp)
    jnh4t=jnh4inp(is)/1000; %g/m2-d
    % compute jn, sod, s
    mmanal2j
    snp(is)=s;

% Compute the dissolved fractions
    fd1m = 1/(1+m1*pi1m);
    fp1m = 1-fd1m;
    fd2m = 1/(1+m2*pi2m);
    fp2m = 1-fd2m;

% Set up the storage for the Mn and alk matrices
    mn = zeros(4,1);
    m = zeros(4);
    fm = zeros(4,1);

% Load matrices
    m(1,1) = -s*fd1m - kmo21 - kl12*fd1m - w12*fp1m;
    m(1,2) = kl12*fd2m + w12*fp2m;
    m(2,1) = kl12*fd1m + w12*fp1m;
    m(2,2) = - kl12*fd2m - w12*fp2m - w2;

```

```

m(3,1) = kmo21;
m(2,4) = kmo22;

m(3,3) = -w12;
m(3,4) = w12;
m(4,3) = w12;
m(4,4) = -kmo22 - w12 - w2;

fm(3) = jmnin;

% Solve for Mn concentrations
mn = -m\fm;

% Compute the fluxes
jmn = s*fd1m*mn(1);
jmnbur = w2*(mn(2)+mn(4));
jnh4(is)=jn*s^2/(s^2+knh41^2)*1000;

% test analytical solution
r12anal=(fd2m*k(12+fp2m*w12)/(fd1m*k(12+kmo21+fd1m*s+fp1m*w12);
r12=mn(1)/mn(2);
mmanal(2)=(jmnin*kmo22)/(w2^2+fd1m*kmo22*s*r12+...
            w2*(kmo21*r12+fd1m*s*r12+kmo22));
mmanal(1)= r12*mmanal(2);
disp(' r12 mn(1) mn(2)')
disp([r12 mn(1) mn(2)])
disp([r12anal mmanal(1) mmanal(2)])

% convert to mg Mn/g, mg Mn/L, mg Mn/m2-d
% Particulate conc. = mg/L /ml (kg/L) * (1 kg/1000g) = mg/g
mnconcp(is,:)=[fp1m*mn(1) fp2m*mn(2) mn(3) mn(4)]./ml ./1000;
mnconct(is,:)=[fp1m*mn(1)+mn(3) fp2m*mn(2)+mn(4)]./ml ./1000;
mnconcd(is,:)=[fd1m*mn(1) fd2m*mn(2)];
flux(is,:)=[jmn jmnbur]*1000;
nflux(is,:)=[jmn/jmnin jmnbur/jmnin];
nfluxapprx(is,:) = s*fd1m*kmo22/(s*fd1m*kmo22 +w2*kmo21);

end % of s loop

% print the results
disp(' ')
disp(' Flux Check')
disp(' flux*[1 1]')
disp(' Particulate Mn and MnO2 Concentrations (mg Mn/g)')
disp(' Particulate Mn (mg Mn/L) and Total Particulate Mn (mg Mn/g)')
disp(' Dissolved Mn (mg Mn/L)')
disp(' Mnconcd; mnconcp;')
disp(' Fluxes: Aqueous, Burial Mn and J[NH4] Fluxes (mg/m2-d)')
disp(' [flux; jnh4]')
disp(' Normalized Fluxes: Aqueous and Burial Mn Fluxes')
disp(' nflux')
disp(' Approx Normalized Mn Flux')
disp(' nfluxapprx')

echo off
% output for systat input
d1=[jnh4;mnconcp;mnconcd;mnconct;flux;nflux]';
save mmanal2.dat d1 /ascii
diary
% pause to examine the printed output
pause
clc
mmanal2p

```



## B. MMANAL2J.M

```

%mmanal2j.m
%Relates jn to jnh4 : parameters are knh41, ao2n=stoichiometric ratio
%
jn = jnh4t/3 + 2*(1/3)*ao2n (2/5)*jnh4t-2/
(3*(2*ao2n-2*jnh4t-3 + 27*jnh4t*knh41-2*o2-2 + ...
3*(3/2)*sqrt(4*ao2n-2*jnh4t-4*knh41-2*o2-2 + ...
27*jnh4t-2*knh41-4*o2-4))^(1/3)) +
(2*ao2n-2*jnh4t-3 + 27*jnh4t*knh41-2*o2-2 + ...
3*(3/2)*sqrt(4*ao2n-2*jnh4t-4*knh41-2*o2-2 + ...
27*jnh4t-2*knh41-4*o2-4))^(1/3)/(3*2^(1/3)*ao2n (2/3));
sod=ao2n*jn;
s=sod/ao2;
% jn*s-2/(s^2+knh41^2)

```

## C. MMANAL2P.M

```

%plot the results - mmanal2p.m
%load the flux data - lis1f -
% J[NH4] J[MN2] (mg/m2-d)
load lis1f.dat;
jmd=lis1f(:,2); jnh4d=lis1f(:,1);
%load the sediment - lismn1 -
% min, max, mean
% ALKPG CAPG NH4PG MMPG CAC03SG MMSG
% (mg CaCO3/L) (mg Ca/L) (mg N/L) (mg Mn/L) (mg CaCO3/g) (mg Mn/g)
load lismn1.dat;
alkpg=lismn1(:,1); capg=lismn1(:,2); nh4pg=lismn1(:,3); mmpg=lismn1(:,4);
cac03sg=lismn1(:,5); mmsg=lismn1(:,6);
jplotd=[1 11.*10];

% Clear the options
clg
%pause(1)
% Normal size
axis('normal')

subplot(221), semilogx(jnh4(:,1),flux(:,1),'-w')
title('Manganese Flux')
xlabel('J[NH4] (mg N/m2-d)')
ylabel('mg Mn/m2-d')
axis('normal')

subplot(222), semilogx(jnh4(:,1),nflux(:,1),'-w',jnh4(:,2),nflux(:,2),'-w')
title('Dissolved (-) and Burial (-)')
xlabel('J[NH4] (mg N/m2-d)')
ylabel('Normalized Flux')

subplot(223), loglog(jnh4(:,2),lismn1(:,2),lismn1(:,4),jmd,'-w',...
jnh4(:,2),lismn1(:,2),lismn1(:,4),jmd,'-w',...
jplotd(3),mmpg(3),'ow',jplotd,mmpg,'-w')
title('Part (-) & Diss. Mn (-)')
xlabel('J[NH4] (mg N/m2-d)')
ylabel('mg Mn/g (x) mg Mn/L (o)')
axis('normal')

subplot(224), loglog(jnh4(:,2),flux(:,1),'-w',jnh4d(:,2),jmd(:,2),'ow')
title('J[Mn] vs J[NH4]')
xlabel('J[NH4] (mg N/m2-d)')
ylabel('J[Mn] (mg Mn/m2-d)')

```

## APPENDIX II

## Model of Calcium Flux - Solubility of CaCO3

```

A. CAALK1.M
clear
diary caalk130.out
echo on
% caalk1.m - 1st version of Ca - Alk - Algebraic solution
% Computed versus jnh4
% -- data plotting for LIS flux data --
echo off
clear
format short e
format compact
echo on
% Define the constants
%Units: mol eq, m, d
m1 = 1; m2 = 1; h2=0.1;
kl12 = 1e-2; w12 = 1.2e-3; w2 = 0.5/365/100;
knh41=0.15; % m/d
o2=5; %g/m3
ao2n=2.54*5.68;
ca0 = 326; alk0=91.8; %mg Ca/L, mg CaCO3/L
jnh4inp = logspace (-1,2,20); %mg/m2-d
kspea = [30];
echo off

%convert olw concs to mol/m3 = mmol/L and eq/m3 = meq/L
ca0=ca0/40; alk0=alk0/50;

% jnh4 loop
for is=1:length(jnh4inp)
jnh4t=jnh4inp(is)/1000; %g/m2-d

%compute jn, sod, s
caalk1j

snp(is)=s;

%Compute alk produced by sulfate reduction - assume all JC goes to SO4 red
%Conversion
%jn (gN/m2-d)/(1000 mgN/gN)*(5.68 gC/gN)
% (1mM C/12 mgC)/(1 meq Alk/1 mM C)*(50 mg CaCO3/meq Alk)
jalkin = (jn*1000)*5.68/12*50; %mg CaCO3/m2-d

%convert alkalinity flux to eq/m2-d
jalkin (mg CaCO3/m2-d)/(1meq/50 mg CaCO3)/(1 mol/1000 mmol)
jalkin=jalkin/50/1000;
jalkinp(is)=jalkin;

%Steady State Solution
caalk1f

%convert to mg /g, mg/L, and mg/m2-d
%Particulate conc:
% (mmol/L) / [(m)(kg/L)] * (1 kg/1000g) * atwt (mg/mmol)= mg/g
%Note: this is a conversion of solid CaCO3 to mg/g
% and at wt for CaCO3 is 100 - not 50.
alkconcp(is,:)=caalk(2j)*100/m1/1000;
cacnconcp(is,:)=caalk(2j)*40/m1/1000;
%Note: this conversion is for dissolved Alk (meq/L)
% to mg CaCO3 equiv /L. Hence, use 50.
alkconcd(is,:)=alkd(1) alkd(2j)*50;

```



```
%mask out the zeros
nfluxp=ones(nflux,nflux);

subplot(221), semilogx(jnh4,flux(:,1),'-w')
title('Alkalinity Flux')
xlabel('J[NH4] (mg/m2-d)')
ylabel('mg CaCO3/m2-d')
axis('normal')

subplot(222), semilogx(jnh4,flux(:,3),'-w',jnh4,flux(:,4),'-w')
title('Calcium Aqueous(-), Burial(...) Flux')
xlabel('J[NH4] (mg/m2-d)')
ylabel('mg Ca/m2-d')
%mask out the zeros
falkconcd=ones(falkconcd)*1e-3;
falkconcd=max(falkconcd,alkconcd);
fcaconcd=ones(fcaconcd)*1e-3;
fcaconcd=max(fcaconcd,caconcd);
subplot(223), loglog(jnh4,falkconcd(:,2),'-w',...
    jnh4,fcaconcd(:,2),'-w',...
    jplotd1(3),alkpg(3),'xw',jplotd1,alkpg,'-w',...
    jplotd2(3),capg(3),'*w',jplotd2,capg,':w')

title('Dissolved Alk(-), Ca(...)')
xlabel('J[NH4] (mg/m2-d)')
ylabel('ALK(x), Ca(*) mg/L')
axis('normal')

%mask out the zeros
falkconcp=ones(falkconcp)*1e-1;
falkconcp=max(falkconcp,alkconcp);
subplot(224), loglog(jnh4,falkconcp(:,1),'-w',...
    jplotd2(3),caco3sg(3),'xw',jplotd2,caco3sg,'-w')

title('Particulate Alk(-)')
xlabel('J[NH4] (mg/g)')
ylabel('ALK(x) mg/g')
meta
```

# APPENDIX III Chemical Model of MnCO3 and CaCO3 Solubility

## A. MNANAL2.M

```
diary mnalcat.t
echo on
% mnalcat.m
% Calculate the solubility for a range of Mn, Alk, and Ca
% Units are mM. Solubility products are (mM^2)
echo off

clear
format short
format compact

kspmn=0.4; kspca=10;

%set alk and mn range for calculation
alkmin=1; alkstep=1; alkmax=20;
mnmin=.05; mnstep=.1; mnmax=.5;
%alk=alkmin:alkstep:alkmax;
%mn=mnmin:mnstep:mnmax;
alk=logspace(log10(alkmin),log10(alkmax),6);
mn=logspace(log10(mnmin),log10(mnmax),6);
%set Ca at LIS conc
ca=300/40;

%storage for solutions
mnalk=zeros(length(alk),length(mn));
caalk=zeros(length(alk),length(mn));

for ialk=1:length(alk)
    for imn=1:length(mn)
        alkt=alk(ialk); mn=mn(imn); cat=ca;
        ksp1=kspmn; ksp2=kspca;

%-- Both MnAlk and CaAlk present
%
mnalk1=alkt*ksp1 - cat*ksp1 + ksp1*mnt + 2*ksp2*mnt;
mnalk2=ksp1*sqrt(alkt^2 - 2*alkt*cat + cat^2 + 4*ksp1 + 4*ksp2 - ...
    2*alkt*mnt + 2*cat*mnt + mnt^2);
mnalk1=(mnalk1-mnalk2)/(2*(ksp1 + ksp2));
caalk1=2*cat*ksp1 + alkt*ksp2 + cat*ksp2 - ksp2*mnt;
caalk2=ksp2*sqrt(alkt^2 - 2*alkt*cat + cat^2 + 4*ksp1 + 4*ksp2 - ...
    2*alkt*mnt + 2*cat*mnt + mnt^2);
caalk1=(caalk1-caalk2)/(2*(ksp1 + ksp2));
mndp1=mnt-mnalk1;
alkdp1=alkt-mnalk1-caalk1;
cadp1=cat-caalk1;

% Negative sign
mnalkm1=(mnalk1-mnalk2)/(2*(ksp1 + ksp2));
caalkm1=(caalk1-caalk2)/(2*(ksp1 + ksp2));
mndm1=mnt-mnalkm1;
alkdm1=alkt-mnalkm1-caalkm1;
cadm1=cat-caalkm1;

%--Only MnAlk present
% Positive sign
mnalkp2=(alkt + mnt + sqrt(alkt^2 + 4*ksp1 - 2*alkt*mnt + mnt^2))/2;
caalkp2=0;
mndp2=mnt-mnalkp2;
alkdp2=alkt-mnalkp2-caalkp2;
cadp2=cat-caalkp2;
```

```

% Negative sign
mna1km2=(alkt + mnt - sqrt(alkt^2 + 4*ksp1 - 2*alkt*mnt + mnt^2))/2;
caalkm2=0;
mndm2=mnt-mna1km2;
alkdm2=alkt-mna1km2-caalkm2;
cadm2=cat-caalkm2;

%-- Only CaAlk present
% Positive sign
caalkp3=(alkt + cat + sqrt(alkt^2 - 2*alkt*cat + cat^2 + 4*ksp2))/2;
mna1kp3=0;
mndp3=mnt-mna1kp3;
alkdp3=alkt-mna1kp3-caalkp3;
cadp3=cat-caalkp3;

% Negative sign
caalkm3=(alkt + cat - sqrt(alkt^2 - 2*alkt*cat + cat^2 + 4*ksp2))/2;
mna1km3=0;
mndm3=mnt-mna1km3;
alkdm3=alkt-mna1km3-caalkm3;
cadm3=cat-caalkm3;

%disp('-----')
%disp('mnt cat alkt')
%disp('mnt cat alktj')
%disp('Solution for both Mna1k and CaAlk present')
%disp('mndm1 mndm1 alkdpl alkdml cadp1 cadm1')
%disp('mndp1 mndm1 alkdpl alkdml cadp1 cadm1')
%disp('mna1kp1 mna1km1 caalkp1 caalkm1')
%disp('mna1kp1 mna1km1 caalkp1 caalkm1')
%disp('Solubility Products')
%disp('[(mndp1)*(alkdp1) (cadp1)*(alkdp1) (mndm1)*(alkdm1) (cadm1)*(alkdm1)]')
%disp('Solution for only Mna1k present')
%disp('mndp2 mndm2 alkdpl alkdml cadp2 cadm2')
%disp('mndp2 mndm2 alkdpl alkdml cadp2 cadm2')
%disp('mna1kp2 mna1km2 caalkp2 caalkm2')
%disp('mna1kp2 mna1km2 caalkp2 caalkm2')
%disp('Solubility Products')
%disp('[(mndp2)*(alkdp2) (cadp2)*(alkdp2) (mndm2)*(alkdm2) (cadm2)*(alkdm2)]')
%disp('Solution for only CaAlk present')
%disp('mndp3 mndm3 alkdpl alkdml cadp3 cadm3')
%disp('mndp3 mndm3 alkdpl alkdml cadp3 cadm3')
%disp('mna1kp3 mna1km3 caalkp3 caalkm3')
%disp('mna1kp3 mna1km3 caalkp3 caalkm3')
%disp('Solubility Products')
%disp('[(mndp3)*(alkdp3) (cadp3)*(alkdp3) (mndm3)*(alkdm3) (cadm3)*(alkdm3)]')

%Select the right solution
mna1kf=0; caalkf=0; chemfini=0; %false - no solution found yet
if ( (mndp1>0) & (cadp1>0) & (alkdp1>0) & (mna1kp1>0) & (caalkp1>0) ...
    & (abs(mndp1*alkdp1)<= ksp1*1e-6) & (abs(cadp1*alkdp1)<= ksp2*1e-6) )
%disp('***MnAlk and CaAlk present - positive solution')
mna1kf=mna1kp1;
caalkf=caalkp1;
chemfini=1;
end
if ( (mndm1>0) & (cadm1>0) & (alkdm1>0) & (mna1km1>0) & (caalkm1>0) ...
    & (abs(mndm1*alkdm1)<= ksp1*1e-6) & (abs(cadm1*alkdm1)<= ksp2*1e-6) )
%disp('***MnAlk and CaAlk present - negative solution')
mna1kf=mna1km1;
caalkf=caalkm1;
chemfini=1;
end
if (~chemfini)

```

```
[0,mm]
disp('Dissolved Alk')
falk,alkdiss]
[0,mm]
disp('Dissolved Ca')
falk,cadiss]
[0,mm]
disp('Percent Mn dissolved')
falk,mmdis./mntot.*100]
[0,mm]
disp('Percent Alk dissolved')
falk,alkdiss./alktot.*100]
[0,mm]
disp('Percent Ca dissolved')
falk,cadiss./catot.*100]
[0,mm]
diary
```

# Model of Manganese Flux - Solubility of MnCO3 and CaCO3

A. MNALCA7.M

```
clear
diary mnalca7.1
%time stamp to id plots
t0 = clock;
str1=[date, ' ', num2str(t0(4)), '-', num2str(t0(5)), '-', num2str(t0(6))];
str2=['Mnalca7.', str1];
echo on
% mnalca7.m - 7th version of Mn - Alk - Ca model - Includes MnO2 -
% Steady State solution - Mathematica
% Computed versus jnh4 - data plotting for LIS flux data
%time Stamp
echo off
disp(str2);

format short e
format compact
%time Stamp

echo on
% Define the constants
m1 = 1; m2 = 1; h2=0.1; h1=0.001;
kl12 = 1e-2; w12 = 1.2e-3; w2 = 0.5/365/100;
kmo21=-.03; kmo22=10; % m/d
jmmo2=0;
fdfs=0;
pil=300;
knh41=0.15; % m/d
o2=5; %g/m3
ao2n=2.54*5.68;
jmmn = 100; jcairn = .001; % mg/m2-d
ca0 = 326; alk0=92; %mg/L
jnh4inp = logspace(0,2,20); %mg/m2-d
%kspminp = [1e-1 1e0 1e1];
kspminp = [0.5];
kspcainp = [20];
echo off

%Units: mol, m, d
%convert fluxes to mol/m2-d
jmmn=jmmn/55/1000; jcairn=jcairn/40/1000;
%convert olw concs to mol/m3 = mmol/L
% 50 mg CaCO3/meq alk
ca0=ca0/40; alk0=alk0/50;

%Calculate fraction dissolved and particulate
fd1=1/(1+m1*pil); fp1=1-fd1;

% output storage
nflux=zeros(length(jnh4inp),6);
flux=zeros(length(jnh4inp),6);
mmconcd=zeros(length(jnh4inp),2);
mmconcp=zeros(length(jnh4inp),3);
caconcd=zeros(length(jnh4inp),2);
caconcp=zeros(length(jnh4inp),1);
alkconcd=zeros(length(jnh4inp),2);
alkconcp=zeros(length(jnh4inp),1);
sinp=zeros(length(jnh4inp),1);
jalkinp=zeros(length(jnh4inp),1);

% solubility loop
```

```

for isol=1:length(kspminp)
kspmn=kspminp(isol);
kspca=kspcainp(1);

% jnh4 loop
for is=1:length(jnh4inp)
%disp('-----')
jnh4=jnh4inp(is)/1000 ; %g/m2-d
%compute jn, sod, s
mmalca7j
slnp(is)=s;

%Compute alk produced by sulfate reduction - assume all JC goes to S04 red
%Conversion
%jn (gN/m2-d)/(1000 mgN/gN)/(5.68 gC/gN)
% (1mM C/12 mgC)/(1 meq Alk/1 mM C)/(50 mg CaCO3/meq Alk)
jalkin = (jn*1000)*5.68/12*50; %mg CaCO3/m2-d

%convert alkalinity flux to eq/m2-d
%jalkin (mg CaCO3/m2-d)/(1meq/50 mg CaCO3)/(1 mol/1000 mmol)
jalkin=jalkin/50/1000;
jalkinp(is)=jalkin;

%Solution
mmalca7f

%substituted version
%disp('Using substituted version')
%mmalca7s

%convert to mg Mn/g, mg CaCO3/g,
mg Mn/L, mg CaCO3/L, mg Ca/L
%
% mg Mn/m2-d, mg CaCO3/m2-d, mg Ca/m2-d

%convert to mg /g, mg/L, and mg/m2-d
%Particulate conc:
% (mmol/L) / [(m1)<(kg/L)] * (1 kg/1000g) * atwt (mg/mmol) = mg/g
mmconcp(is,:)=[mm(3) mm(4) mmalk(2)]*55/m1 /1000;
%Note: this is a conversion of solid CaCO3 to mg/g
% and at wt for CaCO3 is 100 - not 50.
alkconcp(is,:)=[2*mmalk(2)+2*caalk(2)]*100/m1/1000;
caconcp(is,:)=[caalk(2)]*40/m1/1000;
%Note: this conversion is for dissolved Alk (meq/L)
% to mg CaCO3 equiv /L. Hence, use 50.
alkconcd(is,:)=[alk(1) alk(2)-2*caalk(2)-2*mmalk(2)]*50;
caconcd(is,:)=[ca(1) ca(2)-caalk(2)]*40;
mmconcd(is,:)=[mm(1) mm(2)-mmalk(2)]*55;

flux(is,:)=[jmn jmbur jalk jalcabur jca jcabur]*[55 55 50 50 40]*1000;
nflux(is,:)=[jmn/jmbur jalk/jalcabur jca/jcabur]
jalkbur/(jalkin) jca/(jcain) jcabur/(jcain)];
jnh4(is)=jn*s/2/(s*2*knh41*2)*1000;
end % of jnh4 loop

disp(' ')
disp('Elapsed time')
disp(etime(clock,t0))
% print the results
%disp(' Solubility (mM)^2')
%disp(kspmn)
disp(' Flux Check - Mn, Ca, Alk')
%use a matrix product to sum up the fluxes
sflux=sflux*[1 0 0; 1 0 0; 0 1 0; 0 1 0; 0 0 1; 0 0 1];
disp(sflux); % sflux(:,:) sflux(:,:) jalkinp.*50.*1000 1)
disp('Solubility check')
disp(kspmn.*ones(mmconcd(:),2) (mmconcd(:),2) (mmconcd(:),2)./55).*(alkconcd(:),2)./50) ...

```

```

kspca.*ones(mmconcd(:),2) (caconcd(:),2)./40).*(alkconcd(:),2)./50)]
disp(mmconcp)
disp(' Particulate Alk and Ca Concentration (mg CaCO3/g) (mg Ca/g)')
disp(' Particulate Alk and Ca Concentrations (mg/L)')
disp(' Dissolved Mn, Alk, and Ca Concentrations (mg/L)')
disp('mmconcd';alkconcd';caconcd');
disp(' Fluxes: Aqueous and Burial Mn, Alk and Ca Fluxes (mg/m2-d)')
disp('flux')
disp(' Normalized Fluxes: Aqueous and Burial Mn, Alk and Ca Fluxes')
disp('nflux')
disp(' Partition coefficients: Mn, Alk, and Ca (L/kg)')
disp('t(mmconcp(:),3)./mmconcd(:),2).*1000'; ...
(alkconcp./caconcd(:),2).*1000'; ...
(caconcp./caconcd(:),2).*1000);]';
echo off
%output for systat input
d1=[jnh4;mmconcp;alkconcp;caconcp;flux;nflux]';
save mmalca7j.dat d1 /ascii
end % of ksp loop
diary
%pause to examine the printed output
disp('pause')
pause
clc
mmalca7p
-----
B. MNALCA7J.M
%mmalca7j.m
%Relates jn to jnh4t : parameters are knh41, ao2n=stoichiometric ratio
%
jn = jnh4t/3 + 2*(1/3)*ao2n*(2/3)*jnh4t^2/ ...
(3*(2*ao2n^2*jnh4t^3 + 27*jnh4t*knh41^2*ao2^2 + ...
3*(3/2)*sqrt(4*ao2n^2*jnh4t^4*knh41^2*ao2^2 + ...
27*jnh4t^2*knh41^4*ao2^4))^(1/3)) + ...
(2*ao2n^2*jnh4t^3 + 27*jnh4t*knh41^2*ao2^2 + ...
3*(3/2)*sqrt(4*ao2n^2*jnh4t^4*knh41^2*ao2^2 + ...
27*jnh4t^2*knh41^4*ao2^4))^(1/3))/(3*2*(1/3)*ao2n*(2/3));
sod=ao2n*jn;
s=sod/ao2;
% jn*s/2/(s*2*knh41^2)
-----
C. MNALCA7F.M
%Steady State Solution
%mmalca7f.m
ksp1=kspca; ksp2=kspmn;
jalk=jalkin; mn0=jmnin/s;
%Select the right solution - set initially to zero
mmalkf=0; caalkf=0; chemfini=0; %false - no solution found yet
valid=0; %count the no of valid solutions, should be 1
%MnAlk>0 and CaAlk>0
ja0= (alk0 + jalk/kl12 + jalk/s);
jac= (2 - 2*w2/kl12 - 2*w2/s);
jam= (2 - 2*w2/kl12 - 2*w2/s);

```

```

jco= (ca0);
jcc= (1 - w2/kl12 - w2/s);
jmo= ...
((fd1*jmo2*kl12*kmo22 + fd1*jmo2*kmo21*kmo22 + fd1*jmo2*kmo22*mo0*s + ...
fd1*kl12*kmo22*mo0*s + fd1*kmo21*kmo22*mo0*s + ...
fp1*jmo2*kmo22*mo0*s + fd1*kmo22*mo0*s*w12 + fd1*kl12*kmo22*mo0*s*w2 + ...
fp1*mo0*s*w12*w2)/(fd1*kl12*(kmo22*s + kmo21*w2 + s*w2));
jmm= ...
((fd1*kl12*kmo22*s - fdis*fd1*kmo22*s*w12 + fd1*kl12*kmo21*w2 - ...
fd1*kl12*kmo22*w2 - fd1*kmo21*kmo22*mo0*s + fd1*kl12*s*w2 - ...
fdis*fd1*s*w12*w2 - fd1*kl12*w2 - fd1*kmo22*mo0*s*w2 - ...
fd1*s*w2 - fp1*w12*w2 - ...
(fdis*kl12*(kmo22*s + kmo21*w2 + s*w2)));
% Coefficients for mnalk
a= ...
2*ksp1 + 2*jmm*2*ksp1 + jmm*(-4*ksp1 - 2*ksp2) + 2*ksp2 + ...
jcc*(-2*ksp2 + 2*jmm*ksp2);
b= ...
jmo*(-4*ksp1 + 4*jmm*ksp1 - 2*ksp2 + 2*jcc*ksp2) + ...
jco*(2*ksp2 - 2*jmm*ksp2) + ja0*(-ksp2 + jmm*ksp2);
c= ...
-2*jmo*2*ksp1 + ksp2*2 + jmo*(-ja0*ksp2) + 2*jco*ksp2;
%correct for the c being on the rhs in mncaal8g
c=-c;
%Positive and negative solutions
mnalkp=(-b+sqrt(b^2-4*a*c))/(2*a);
mnaln=(-b-sqrt(b^2-4*a*c))/(2*a);
%Check the equations
mnalkp= ...
2*jco*jmm*ksp1 + 4*jmm*jmo*ksp1 - ja0*ksp2 + 2*jco*ksp2 + ja0*jmm*ksp2 - ...
(2*ksp1 - 4*jmm*ksp1 + 2*jmo*ksp2 + 2*jcc*jmo*ksp2)*mnalkp + ...
2*jmm*ksp2 + 2*jcc*jmm*ksp2)*mnalkp - 2*jcc*ksp2 - ...
-2*jmo*2*ksp1 - ja0*jmo*ksp2 + 2*jco*jmo*ksp2 + ksp2*2);
%Negative Roots
%disp('Mnalk>0, CaAlk>0 - Negative roots')
mnalk=mnaln;
%Coefficients for caalk
a=2 - 4*jcc + 2*jcc^2;
b=ja0*(-1 + jcc) + (-2 + 2*jcc)*jco + 2*mnalk - 4*jcc*mnalk + 2*jcc^2*mnalk;
c=-(ja0*jco) + ksp1 + jco*(2*mnalk - 2*jcc*mnalk);
%correct for the c being on the rhs in mncaal8g
c=-c;
%negative solution
caalkn=(-b+sqrt(b^2-4*a*c))/(2*a);
caalk=caaln;
%Check the equations
caalkn=2*(2 - 4*jcc + 2*jcc^2) + ...
caalk*(-ja0 + ja0*jcc - 2*jco + 2*jcc*jco + 2*mnalkn - 4*jcc*mnalkn + ...
2*jcc^2*mnalkn) - ...
-(ja0*jcc + ksp1 + 2*jco*mnalkn - 2*jcc*jco*mnalkn);
%Evaluate Layer 1 and 2 solutions and check feasibility
mnalca7g
%Positive Roots
%disp('Mnalk>0, CaAlk>0 - Positive roots')
mnalk=mnalkp;

```

```

%Coefficients for caalk
a=2 - 4*jcc + 2*jcc^2;
b=ja0*(-1 + jcc) + (-2 + 2*jcc)*jco + 2*mnalk - 4*jcc*mnalk + 2*jcc^2*mnalk;
c=-(ja0*jco) + ksp1 + jco*(2*mnalk - 2*jcc*mnalk);
%correct for the c being on the rhs in mncaal8g
c=-c;
%Positive solution
caalkp=(-b+sqrt(b^2-4*a*c))/(2*a);
caalk=caalkp;
%Check the equations
caalkp=2*(2 - 4*jcc + 2*jcc^2) + ...
caalk*(-ja0 + ja0*jcc - 2*jco + 2*jcc*jco + 2*mnalkp - 4*jcc*mnalkp + ...
2*jcc^2*mnalkp) - ...
-(ja0*jcc + ksp1 + 2*jco*mnalkp - 2*jcc*jco*mnalkp);
%Evaluate Layer 1 and 2 solutions
mnalca7g
%The caalk=0 case
caalk=0;
%Zero the caalk dependent terms
ja0= (alk0 + jalk/kl12 + jalk/s);
jac= (2 - 2*w2/kl12 - 2*w2/s);
jam= (2 - 2*w2/kl12 - 2*w2/s);
jco= (ca0);
jcc= (1 - w2/kl12 - w2/s);
jmo= ...
((fd1*jmo2*kl12*kmo22 + fd1*jmo2*kmo21*kmo22 + fd1*jmo2*kmo22*mo0*s + ...
fd1*kl12*kmo22*mo0*s + fd1*kmo21*kmo22*mo0*s + ...
fp1*jmo2*kmo22*mo0*s + fd1*kl12*(kmo22*s + kmo21*w2 + s*w2));
jmm= ...
((fd1*kl12*kmo22*s - fdis*fd1*kmo22*s*w12 + fd1*kl12*kmo21*w2 - ...
fd1*kl12*kmo22*w2 - fd1*kmo21*kmo22*mo0*s + fd1*kl12*s*w2 - ...
fdis*fd1*s*w12*w2 - fd1*kl12*w2 - fd1*kmo22*mo0*s*w2 - ...
fd1*s*w2 - fp1*w12*w2 - ...
(fdis*kl12*(kmo22*s + kmo21*w2 + s*w2)));
% Coefficients for mnalk
a=2 - jam + (-2 + jam)*jmm;
b=ja0*(-1 + jmm) + (-2 + jam)*jmo;
c=-(ja0*jmo) + ksp2;
%correct for the c being on the rhs in mncaal8g
c=-c;
%Positive and negative solutions
mnalkp=(-b+sqrt(b^2-4*a*c))/(2*a);
mnaln=(-b-sqrt(b^2-4*a*c))/(2*a);
%Check the equations
mnalkp= ...
(-ja0 + ja0*jmm - 2*jmo + jam*jmo)*mnalk + ...
(2 - jam - 2*jmm + jam*jmm)*mnalk - 2*(-ja0*jmo) + ksp2);
%Negative Roots
%disp('Mnalk>0, CaAlk=0 - Negative roots')
mnalk=mnaln;
%Evaluate Layer 1 and 2 solutions and check feasibility
mnalca7g
%Positive Roots
%disp('Mnalk>0, CaAlk=0 - Positive roots')
mnalk=mnalkp;

```

%Evaluate Layer 1 and 2 solutions and check feasibility

mmalca7g

%The mnalk=0 case

mnalk=0;

ja0= (alk0 + jalk/kl12 + jalk/s);

jac= (2 - 2\*w2/kl12 - 2\*w2/s);

jmn= (2 - 2\*w2/kl12 - 2\*w2/s);

jco= (ca0);

jcc= (1 - w2/kl12 - w2/s);

jmo=

((fd1\*jmo2\*kl12\*kmo22 + fd1\*jmo2\*kmo21\*kmo22 + fd1\*jmo2\*kmo22\*s + ...  
fd1\*kl12\*kmo22\*mn0\*s + fd1\*kmo21\*kmo22\*mn0\*s + ...  
fp1\*jmo2\*kmo22\*w12 + fp1\*kmo22\*mn0\*s\*w12 + fd1\*kl12\*mn0\*s\*w2 + ...  
fp1\*mn0\*s\*w12\*w2)/(fd1\*kl12\*(kmo22\*s + kmo21\*w2 + s\*w2)));

jmn= ((fd1\*kl12\*kmo22\*s - fdis\*fd1\*kmo22\*s\*w12 + fd1\*kl12\*kmo21\*w2 - ...  
fd1\*kl12\*kmo22\*w2 - fd1\*kmo21\*kmo22\*w2 + fd1\*kl12\*s\*w2 - ...  
fd1\*kmo22\*s\*w2 - fdis\*fd1\*kmo21\*w12\*w2 - fp1\*kmo22\*w12\*w2 - ...  
fdis\*fd1\*s\*w12\*w2 - fd1\*kl12\*w2 - fd1\*kmo21\*w2 - ...  
fd1\*s\*w2 - fp1\*w12\*w2)/...  
(fd1\*kl12\*(kmo22\*s + kmo21\*w2 + s\*w2)));

%Coefficients for caalk

a=2 - jac + (-2 + jac)\*jcc;

b=ja0\*(-1 + jcc) + (-2 + jac)\*jco;

c=(-ja0\*jco) + ksp1;

%correct for the c being on the rhs in mncaal8g  
c=-c;

%positive and negative solutions

caalk=(-b+sqrt(b^2-4\*a\*c))/(2\*a);

caalkn=(-b-sqrt(b^2-4\*a\*c))/(2\*a);

%Negative Root

%disp('MnAlk=0, CaAlk>0 - Negative roots')

caalk=caalkn;

%Check the equation

caalk\*2\*(2 - jac - 2\*jcc + jac\*jcc) + ...;

caalk\*(-ja0 + ja0\*jcc - 2\*jco + jac\*jco) - (-ja0\*jco) + ksp1);

%Evaluate Layer 1 and 2 solutions and check feasibility

mmalca7g

%Positive Root

%disp('MnAlk=0, CaAlk>0 - Positive roots')

caalk=caalkp;

%Check the equation

caalk\*2\*(2 - jac - 2\*jcc + jac\*jcc) + ...;

caalk\*(-ja0 + ja0\*jcc - 2\*jco + jac\*jco) - (-ja0\*jco) + ksp1);

%Evaluate Layer 1 and 2 solutions and check feasibility

mmalca7g

%Check that no more than 1 valid solution found

if(valid>1)

disp('More than 1 valid solution')

end

%Rest of the variables

mnalk=mnalkf;

caalk=caalkf;

%Evaluate Layer 1 and 2 solutions

mmalca7g

mnalk(2)=mnalkf;

caalk(2)=caalkf;

mnaldis=mn2-mnalkf;

cadiss=ca2-caalkf;  
alkdis=alk2-2\*caalkf-2\*mnalkf;  
%disp('mnalkf caalkf mndiss cadiss alkdiss')  
%disp('mnalkf caalkf mndiss cadiss alkdiss')  
%disp('kspm mndiss\*alkdiss kspca cadiss\*alkdiss mnalkf caalkf')  
%disp('kspm mndiss\*alkdiss kspca cadiss\*alkdiss mnalkf caalkf')

%Print  
%if( (it-tprint\*round(it/tprint))==0 );

%disp('Solubility from Chem')

%disp('kspm mndiss\*alkdiss kspca cadiss\*alkdiss mnalkf caalkf')

%end

%store the results

alk(l1 2)=falk1,alk2;

ca(l1 2)=[ca1,ca2];

mn(l1 2 3 4)=lmm1,mn2,mno21,mno22;

mnalk(2)=mnalkf;

caalk(2)=caalkf;

%Fluxes

jalksav=jalk; %save source

jalk = s\*(alk(1)-alk0);

jalkbur=2\*w2\*(caalk(2)+mnalk(2));

jcas=s\*(ca(1)-ca0);

jcabur=w2\*caalk(2);

jmn = s\*fd1\*mn(1);

jmbur=w2\*(mnalk(2)+mn(4));

%Final equation check

e1=...  
kl12\*(-alk1 + alk2 - 2\*caalkf - 2\*mnalkf) - (-alk0 + alk1)\*s;

e2=...  
jalksav - kl12\*(-alk1 + alk2 - 2\*caalkf - 2\*mnalkf) - (2\*caalkf + 2\*mnalkf)\*w2;

e3=...  
(-caalkf - ca1 + ca2)\*kl12 + ca0\*s - ca1\*s;

e4=...  
-((-caalkf - ca1 + ca2)\*kl12) - caalkf\*w2;

e5=...  
-ksp1 + (-caalkf + ca2)\*(alk2 - 2\*caalkf - 2\*mnalkf);

e6=...  
-(fd1\*kmo21\*mn1) + kl12\*(-mnalkf - fd1\*mn1 + mn2) - (-mn0 + fd1\*mn1)\*s + ...

(fdis\*mnalkf - fp1\*mn1)\*w12;

e7=...  
kmo22\*mno22 - kl12\*(-mnalkf - fd1\*mn1 + mn2) - (fdis\*mnalkf - fp1\*mn1)\*w12 - ...

mnalkf\*w2;

e8=...  
-ksp2 + (alk2 - 2\*caalkf - 2\*mnalkf)\*(-mnalkf + mn2);

e9=...  
jmo2 + fd1\*kmo21\*mn1 + (-mno21 + mno22)\*w12;

e10=...  
-(kmo22\*mno22) - (-mno21 + mno22)\*w12 - mno22\*w2;

%Generate the Maximum mass balance error

err=max(abs([e1,e2,e3,e4,e6,e7,e9,e10]));

if(err>1e-10)

disp('MB Error exceeded')

[jnh4,e1,e2,e3,e4,e6,e7,e9,e10]

end

-----

D. MNALCA7G.M

%MnAlca7g.m - Layer 1 and 2 solutions



```

%Layer 2
alk2= ...
(alk0 + 2*caalk + jalk/kl12 + 2*mmalk + jalk/s - 2*caalk*w2/kl12 - ...
2*mmalk*w2/kl12 - 2*caalk*w2/s - 2*mmalk*w2/s);
ca2= ...
(caalk + ca0 - caalk*w2/kl12 - caalk*w2/s);
mm2= ...
((fd1*jmo2*k12*kmo22 + fd1*jmo2*kmo21*kmo22 + fd1*jmo2*kmo22*s + ...
fd1*k12*kmo22*mmalk*s + fd1*k12*kmo22*mm0*s + ...
fd1*kmo21*kmo22*mm0*s + fp1*jmo2*kmo22*mm0*s + ...
fd1*k12*kmo22*mmalk*s*w12 + fp1*kmo22*mm0*s*w12 + ...
fd1*k12*kmo21*mmalk*w2 - fd1*k12*kmo22*mmalk*w2 - ...
fd1*kmo21*kmo22*mmalk*w2 + fd1*k12*mmalk*s*w2 - ...
fd1*kmo22*mmalk*s*w2 + fd1*k12*mm0*s*w2 - ...
fd1*kmo21*mmalk*w12*w2 - fp1*kmo22*mmalk*w12*w2 - ...
fd1*k12*mmalk*s*w12*w2 + fp1*mm0*s*w12*w2 - ...
fd1*k12*mmalk*w2*2 - fd1*kmo21*mmalk*w2*2 - ...
fd1*mmalk*s*w2*2 - fp1*mmalk*w12*w2*2)/ ...
(fdi*k12*(kmo22*s + kmo21*w2 + s*w2));
mm021= ...
((kmo22 + w12 + w2)*(jmo2*kmo21 + jmo2*s + kmo21*mm0*s - ...
kmo21*mmalk*w2)/(w12*(kmo22*s + kmo21*w2 + s*w2));
mm022= ...
((jmo2*kmo21 + jmo2*s + kmo21*mm0*s - kmo21*mmalk*w2)/ ...
(kmo22*s + kmo21*w2 + s*w2));
%Layer 1
alk1= ...
(alk2*k12 - 2*caalk*k12 - 2*k12*mmalk + alk0*s)/(k12 + s);
cal= ...
((-caalk*k12) + ca2*k12 + ca0*s)/(k12 + s);
mm1= ...
((-k12*mmalk) + k12*mm2 + mm0*s + fdis*mmalk*w12)/ ...
(fdi*k12 + fd1*kmo21 + fd1*s + fp1*w12);
e5= ...
-ksp1 + (-caalk + ca2)*(alk2 - 2*caalk - 2*mmalk);
e8= ...
-ksp2 + (alk2 - 2*caalk - 2*mmalk)*(mmalk + mm2);
%Check feasibility of solution
mm2d=mm2-mmalk;
alk2d=alk2-2*mmalk-2*caalk;
ca2d=ca2-caalk;
%disp([kspmm mm2d*alk2d kspca ca2d*alk2d mmalk caalk])
DisPos=(mm2d>0)&(alk2d>0)&(ca2d>0);
SolidPos=(mmalk>0)&(caalk>0);
OverSat=((kspmm+1e-6)<(mm2d*alk2d))/((kspca+1e-6)<(ca2d*alk2d));
UnderSat=OverSat;
ValidSol=(DisPos&SolidPos&UnderSat);
%disp([DisPos SolidPos ValidSol])
%disp([DisPos SolidPos ValidSol])
if(ValidSol, valid=valid+1, end;
if(ValidSol)
mmalkf=mmalk;
caalkf=caalk;
chemfini=1;
end
E. MNALCA7P.M
%Plot the results
%mmalca7p.m

```

```

% Clear the options
clg
%pause(1)
% Normal size

%Load the flux data - listf -
% J[NH4] J[MN2] (mg/m2-d)
load listf.dat;
jmh4=listf(:,2); jmh4d=listf(:,1);
%Load the sediment - listm1 -
% min, max, mean
% ALKPG, CAPG NH4PG MHPG CAC03SG MMSG
% (mg CaCO3/L) (mg Ca/L) (mg N/L) (mg Mn/L) (mg CaCO3/g) (mg Mn/g)
load listm1.dat;
alkpg=listm1(:,1); capg=listm1(:,2); nh4pg=listm1(:,3); mmpg=listm1(:,4);
cac03sg=listm1(:,5); mmsg=listm1(:,6);
splotd=[1 1 1]*.3; splotd2=[1 1 1]*.5; splotd2=[1 1 1]*.10;

axis('normal')
%mask out the zeros
nfluxp=ones(nflux)*1e-3;
nfluxp=max(nflux,nfluxp);
subplot(221), semilogx(jnh4(:),nfluxp(:),1,'-w',jnh4(:),nfluxp(:),3,'--w')
xlabel('J[NH4] (mg N/m2-d)')
ylabel('Mn(-) N Flux')

axis('normal')
%mask out the zeros
fluxp=ones(flux)*1e-3;
fluxp=max(flux,fluxp);
subplot(222), loglog(jnh4(:),fluxp(:),1,'-w',jnh4(:),fluxp(:),3,'--w',...
ylabel('J[Mn(-) JALK(-) mg/m2-d')
xlabel('J[NH4] (mg N/m2-d)')

%Title
text(0.3,1,str2,'sc');

%mask out the zeros
fmmconcd=ones(fmmconcd)*1e-3;
fmmconcd=max(fmmconcd,fmmconcd);
falkconcd=ones(falkconcd)*1e-3;
falkconcd=max(falkconcd,falkconcd);
fcaconcd=ones(fcaconcd)*1e-3;
fcaconcd=max(fcaconcd,fcaconcd);
subplot(223), loglog(jnh4(:),fmmconcd(:),2,'-w',jnh4(:),falkconcd(:),2,'--w',...
jnh4(:),fcaconcd(:),2,'-w',...
splotd(3),mmpg(3),'ow',splotd,mmpg,'-w',...
splotd(3),alkpg(3),'xw',splotd1,alkpg,'--w',...
splotd2(3),capg(3),'w',splotd2,capg,':w')

title(' Diss. Mn(-), Alk(-), Ca(+)')
xlabel('J[NH4] (mg N/m2-d)')
ylabel('Mn(o), Alk(x), Ca(*) mg/L')

axis('normal')
%mask out the zeros
fmmconcp=ones(fmmconcp)*1e-3;
fmmconcp=max(fmmconcp,fmmconcp);
falkconcp=ones(falkconcp)*1e-3;
falkconcp=max(falkconcp,falkconcp);
fcaconcp=ones(fcaconcp)*1e-3;
fcaconcp=max(fcaconcp,fcaconcp);
subplot(224), loglog(jnh4(:),fmmconcp(:),3,'-w',jnh4(:),falkconcp(:),1,'--w',...

```

```

    splotd(3),mmsg(3),'ow',splotd,mmsg,'-w',...
    splotd(3),caco3sg(3),'xw',splotd2,caco3sg,'-w')
title('Part. Mn(-), Alk (- -)')
xlabel('J[NH4] (mg N/m2-d)')
ylabel('mg Mn/g (o) mg Alk/g (x)')

pause
clg

subplot(221), semilogx(jnh4(:),fluxp(:,1),'-w')
xlabel('J[NH4] (mg N/m2-d)')
ylabel('J[Mn] mg Mn/m2-d')
axis('normal')

%Title
text(0.3,1,str2,'sc');

subplot(222), semilogx(jnh4(:),nfluxp(:,1),'-w',jnh4(:),nfluxp(:,2),'-w')
ylabel('Diss (-), Burial (- -)')
xlabel('J[NH4] (mg N/m2-d)')

subplot(223), loglog(jnh4(:),[mnconcp(:,2)+mnconcp(:,3)],'-w',...
    jnh4(:),mnconcp(:,2),'-w',...
    splotd(3),mmsg(3),'ow',splotd,mmsg,'-w',...
    splotd(3),mmsg(3),'xw',splotd,mmsg,'-w')
title('Part (-) & Diss. Mn (- -)')
xlabel('s (m/d)')
ylabel('mg Mn/g (x) mg Mn/L (o)')
axis('normal')

subplot(224), loglog(jnh4(:),fluxp(:,1),'-w',jnh4(:),jmd(:,1),'ow')
title('J[Mn] vs J[NH4]')
xlabel('J[NH4] (mg N/m2-d)')
ylabel('J[Mn] (mg Mn/m2-d)')

```

# REPORT DOCUMENTATION PAGE

Form Approved  
OMB No. 0704-0188

Public reporting burden for this collection of information is estimated to average 1 hour per response, including the time for reviewing instructions, searching existing data sources, gathering and maintaining the data needed, and completing and reviewing the collection of information. Send comments regarding this burden estimate or any other aspect of this collection of information, including suggestions for reducing this burden, to Washington Headquarters Services, Directorate for Information Operations and Reports, 1215 Jefferson Davis Highway, Suite 1204, Arlington, VA 22202-4302, and to the Office of Management and Budget, Paperwork Reduction Project (0704-0188), Washington, DC 20503.

1. AGENCY USE ONLY (Leave blank)	2. REPORT DATE July 1994	3. REPORT TYPE AND DATES COVERED Final report	
4. TITLE AND SUBTITLE A Model of Manganese and Iron Fluxes from Sediments		5. FUNDING NUMBERS	
6. AUTHOR(S) Dominic M. Di Toro, James F. Fitzpatrick, Richard R. Isleib			
7. PERFORMING ORGANIZATION NAME(S) AND ADDRESS(ES) HydroQual, Inc. One Lethbridge Plaza Mahwah, NJ 07430		8. PERFORMING ORGANIZATION REPORT NUMBER	
9. SPONSORING/MONITORING AGENCY NAME(S) AND ADDRESS(ES) U.S. Army Corps of Engineers, Washington, DC 20314-1000; U.S. Army Engineer Waterways Experiment Station, 3909 Halls Ferry Road, Vicksburg, MS 39180-6199		10. SPONSORING/MONITORING AGENCY REPORT NUMBER Contract Report W-94-1	
11. SUPPLEMENTARY NOTES Available from National Technical Information Service, 5285 Port Royal Road, Springfield, VA 22161.			
12a. DISTRIBUTION/AVAILABILITY STATEMENT Approved for public release; distribution is unlimited.		12b. DISTRIBUTION CODE	
13. ABSTRACT (Maximum 200 words)  Iron and manganese are installed as state variables in a previously developed benthic sediment model. Initial emphasis is placed on manganese because of availability of observations. Mass-balance and chemical equilibrium equations for manganese in benthic sediments are presented. The model is tested in steady-state and time-variable mode against observations collected in Long Island Sound and Narragansett Bay. The initial model captures seasonal trends in sediment manganese release, although the magnitude of seasonal variability is underestimated. Improvement of the model through representation of manganese carbonate solubility is recommended.			
14. SUBJECT TERMS Iron                                      Model Manganese                              Sediments		15. NUMBER OF PAGES 76	
		16. PRICE CODE	
17. SECURITY CLASSIFICATION OF REPORT UNCLASSIFIED	18. SECURITY CLASSIFICATION OF THIS PAGE UNCLASSIFIED	19. SECURITY CLASSIFICATION OF ABSTRACT	20. LIMITATION OF ABSTRACT